We noticed in microarray analysis that RORC, the human ortholog of murine RORγt, a major transcription factor for Th17 cell differentiation (Ivanov et al., 2006), was highly upregulated in both Fr. II and III and much less in Fr. I. Indeed, FoxP3^{lo} memory-like non-Tregs (Fr. III) were the highest producers of IL-17 among CD4$^+$ T cells. These results support recent findings in mice that FoxP3-RORγt double-positive CD4$^+$ T cells can convert into either Treg cells or Th17 cells (Yang et al., 2008a; Zhou et al., 2008). AHR was recently shown in mice to be critical for the differentiation of naive T cells to Th17 versus FoxP3$^+$ Treg cells (Quintana et al., 2008; Veldhoen et al., 2008). Our finding of upregulated AHR repressor in aTreg cells therefore suggests that differentiation of FoxP3$^-$CD4$^+$ T cells to aTreg cells might be regulated through the modulation of AHR activity by AHR repressor. Further study is required to determine how the expression amount of FoxP3 in each FoxP3$^+$ subpopulation contributes to the function of each subset (e.g., suppression and IL-17 production) through interaction with other molecules including RORC.

This study has revealed several key features of Treg cell-mediated suppression in vitro. First, challenging the commonly accepted notion that Treg cells are anergic in vitro, human Treg cells proliferate and die, although the degree of their proliferation is much lower than that of non-Treg cells when Treg cells and non-Treg cells are separately stimulated and compared. Further, the hypoproliferation observed with CD25^{hi}CD4$^+$ T cells can be attributed, in part, to the suppression of rTreg cell proliferation by aTreg cells and also to the death of the latter. These findings mean that thymidine uptake by whole cocultured cells in Treg cell assay may not be accurate to monitor responder cell proliferation in the presence of Treg cells. Second, CTLA-4 expression in aTreg cells, but not in rTreg cells, suggests that aTreg cells are the main effectors of suppression as shown by the fact that Treg cell-specific deficiency impairs Treg cell suppressive function in vivo and in vitro in mice (Wing et al., 2008). Further, FoxP3$^+$ Treg cells out-compete naive T cells in in vitro aggregation around dendritic cells and downregulate their expression of CD80 and CD86 in a CTLA-4-dependent fashion (Onishi et al., 2008). It is likely in humans that, upon activation, rTreg cells differentiate to aTreg cells and exert suppression in vitro through these mechanisms. As another possibility, rTreg and aTreg cells might use different suppressive mechanisms by secreting different immunosuppressive cytokines such as IL-10 and TGF-β (Ito et al., 2008). Our microarray analysis indeed indicates that aTreg cells are more active in IL-10 transcription but less active in TGF-β transcription than rTreg cells. Further study is required to determine whether Treg cells use multiple suppressive mechanisms depending on their differentiation status (Sakaguchi et al., 2008).

Finally, supporting physiological and clinical relevance of distinguishing subpopulations of FoxP3$^+$ T cells, rTreg and aTreg cells can be clearly identified with different proportions in cord blood of healthy newborns, PBL of aged individuals, and patients with SLE or sarcoidosis. In cord blood, we unexpectedly found a small but always detectable population of CD45RA^{lo}Ki-67$^+$FoxP3^{hi}CD4$^+$ T cells that corresponded to adult aTreg cells. This finding suggests that even in fetuses, natural rTreg cells are constantly activated by endogenous self antigens and exogenous antigens derived from maternal circulation. An opposite trend exists in aged donors, who had high proportions of aTreg cells and low but still detectable proportions of rTreg cells. Because of thymus involution observed in aged individuals, one can speculate that, like conventional naive CD4$^+$ T cells (Vrisekoop et al., 2008), rTreg cells can be generated in the periphery in aged individuals to compensate for decreased thymic production of Treg cells; alternatively, but not exclusively, aTreg cells may homeostatically expand to counterbalance the lack of rTreg cells in the periphery. Under pathological conditions, a high prevalence of aTreg cells and a decrease in the rTreg cell population in sarcoidosis suggests that rTreg cells may be swiftly converted into aTreg cells immediately after having emigrated from the thymus or having been peripherally generated. In contrast, in active SLE, the number of aTreg cells decreased while that of rTreg cells remained normal or increased, with a notable increase in FoxP3^{lo}CD4$^+$ non-Treg cells. This also confirms the FoxP3^{lo}CD45RA$^-$ memory/effector-like non-Treg cell subset as a discrete population among FoxP3$^+$ CD4$^+$ T cells. Further functional analysis is required to interpret these anomalies and variations in disease states (Taflin et al., 2009). Yet, analysis of Treg cell function by dissecting FoxP3$^+$ cells into three subpopulations is instrumental for understanding pathophysiology of immunological diseases.

In conclusion, we propose a definition of human FoxP3$^+$ Treg cell subsets based on in vitro and in vivo features of FoxP3-expressing CD4$^+$ T cells. Functional and numerical analysis of each subset will help to understand and control immune responses in normal and disease states.

EXPERIMENTAL PROCEDURES

Human Samples

Blood samples were obtained from young healthy adult volunteers (18–40 years old), from aged control donors (79–90 years old), and from active sarcoidosis or active SLE patients and cord blood samples from full-term neonates who had no hereditary disorders, hematologic abnormalities, or infectious complications. Aged donors had no acute or chronic inflammatory or infectious disease, ongoing thrombosis, or neoplasia. Diagnosis of active SLE and sarcoidosis were made according to previously described criteria (Miyara et al., 2005, 2006). All patients were newly diagnosed and not medicated with steroid or immunosuppressant. The study was done according to the Helsinki declaration with the approval from the human ethics committee of the Institute for Frontier Medical Sciences, Kyoto University and from Comité Consultatif de Protection des Personnes dans la Recherche Biomédicale of Pitié-Salpétrière Hospital, Paris. Human peripheral blood PBMC were prepared by Ficoll gradient centrifugation. Lymphocyte subpopulations was isolated by a MoFLo cell sorter (Dako) after positive magnetic cell separation of CD4$^+$ T cells by CD4$^+$ T cell MACS beads (Miltenyi Biotec). Purity of isolated cells was always >95% (Figure S1). Autologous CD14$^+$ and CD19$^+$ cells positively selected by mixed MACS and irradiated (50 Gy) were used as accessory cells.

Mice

NOG mice described previously (Hiramatsu et al., 2003) were injected intravenously with 3.5–5 × 10^7 human PBMCs. The mice were maintained in our animal facility and treated in accordance with the guidelines of Kyoto University.

Flow Cytometry

Freshly obtained or in vitro cultured lymphocytes and human lymphocytes isolated from NOG mouse spleens were stained with anti-hCD4 (-PerCP-Cy5.5 from BD biosciences or -APC from R&D Systems), anti-hCD25 (-PE or -PE-Cy5 from BD), anti-hCD45RO (-PE from Beckman Coulter and PE-Cy7 from

BD), anti-hCD45RA (-PE-Cy7 from BD or -FITC from Beckman Coulter), anti-ICOS (-FITC from e-Bioscience), anti-HLA-DR (-PE from BD biosciences), anti-CD31 (-APC from e-Bioscience), anti-hCD127 (-PE from Beckman Coulter and -PE-Cy5 from e-bioscience), and 7-AAD (Dako). Intracellular detection of FoxP3 with anti-hFoxP3 (PE or Alexa Fluor 647, clone 236A/E7 [e-Bioscience] or clone 259D [BD biosciences]) and of Ki-67 antigen with Ki-67 antibody (FITC or PE from BD) was performed on fixed and permeabilized cells via Cytofix/Cytoperm (e-Bioscience). For detection of intracellular cytokine production, $CD4^+$ T cells were stimulated with 20 ng/ml PMA and 1 μM ionomycin in the presence of Golgi-Stop (BD Biosciences) for 5 hr and then stained with anti-hFoxP3-PE, Ki-67-FITC, anti-IL2-APC (BD Biosciences), anti-IFN-γ-APC (BD), or anti-IL-17-Alexa Fluor 647 (e-Bioscience) after fixation and permeabilization. Data acquired by FACSCalibur (Becton Dickinson) were analyzed with WinMDI 2.9 software (http://facs.scripps.edu/software.html). Statistical comparisons were performed with the nonparametric Mann-Whitney U test.

Cell Culture and Suppression Assay

RPMI 1640 medium supplemented with 10% fetal bovine serum, 100 IU/ml penicillin, and 100 μg/ml streptomycin (Sigma, St. Louis, MO) was used for T cell culture. Cells were labeled with 1 μM CFSE (Dojindo and Invitrogen). In suppression assays, unless otherwise indicated, 1×10^4 CFSE-labeled responder $CD25^-CD45RA^+CD4^+$ T cells were cocultured with 1×10^4 unlabeled cells assessed for their suppressive capacity and 1×10^5 irradiated autologous accessory cells and were stimulated with 0.5 μg/mL plate-bound anti-CD3 (OKT3 mAb) in 96-well round-bottom plate in supplemented RPMI medium. Proliferation of CFSE-labeled cells was assessed by flow cytometry after 84–90 hr of culture. Percent suppression was calculated by dividing the number of proliferating CFSE-diluting responder cells in the presence of suppressor cells at a 1 to 1 ratio by the number of proliferating responder cells when cultured alone, and multiplied by 100.

FOXP3 Gene DNA Methylation

The genomic DNA from purified human $CD4^+$ T cell subsets was extracted by the Blood & Tissue Genomic DNA Extraction System (Viogene). Genomic DNA from purified cells was bisulfite converted by the EpiTect Bisulfite Kit (QIAGEN) according to the manufacturer's instructions. DNA was then subjected to PCR with primers for amplification of specific targets in bisulfite-treated DNA. The PCR products obtained were cloned into the pGEM-T Easy vector (Promega) and 20 individual clones from each sample were cycle sequenced by the BigDye Terminator kit (ver. 3.1; Applied Biosystems) and the ABI automated DNA sequencer (Applied Biosystems). Primers used: Fxpro-met_F1, 5′-TTTTT GTGGTGAGGGGAAGAAATTATATT-3′; Fxpro-met_R2, 5′-TACCATCTCCTC CAATAAAACCCACATC-3′; Fxint-met_F8, 5′-TTTGGGTTAAGTTTGTTGTAG GATAGGGTAGTTAG-3′; Fxint-met_R7, 5′-AAATCTACATCTAAACCCTATTAT CACAACCCC-3′.

Single Cell Sorting, RT-PCR, and Vβ5 Sequence Analysis

PBLs were stained with anti-human CD4-FITC, anti-human CD25-PC7 (BD Biosciences), and anti-human BV5.1, BV5.2, BV5.3-PPE (Beckman Coulter). Single cells were sorted with the FACS Vantage (Becton Dickinson) into 96-well PCR plates (Abgene, Epsom). Single-cell RT-PCR conditions were as previously described (Miyara et al., 2006). In the first PCR round, BV5ext (5′-GATCAAAACGAGAGGACAGC-3′) and BC (5′-CGGGCTGCTCCTTGAG GGGCTGCG-3′) were used. Reactions were subjected after 5 min at 94°C to 8 cycles (94°C for 30 s, 60°C for 40 s, 72°C for 50 s), 32 cycles (94°C for 30 s, 55°C for 40 s, 72°C for 50 s), and a final elongation at 72°C for 5 min. In a second PCR round, nested primers BV5 (5′-AGCTCTGAGCTGAATGT GAACGCC-3′) and BC-int (5′-GCGGGTCYGTGCTGACCC-3′) were used. PCR was performed as in the first step.

Products were subjected to automated sequencing (ABI 3100, Applied Biosystems).

Specific questions regarding this repertoire analysis should be sent to guy.gorochov@upmc.fr.

Microarray and Real-Time PCR

RNA was extracted from FACS-sorted $CD4^+$ T cells according to their amounts of CD25 and CD45RA and analyzed by Affymetrix Human Genome U133 Plus 2.0 Arrays.

Real-time PCR was performed with a SYBR green assay on the LightCycler 480 system (Roche). Total RNA extracted from FACS-sorted T cells was reverse transcribed according to the manufacturer's instructions (RNeasy Micro kit, QIAGEN). In each reaction, hypoxanthine phosphoribosyltransferase-1 (HPRT-1) was amplified as a housekeeping gene to calculate a standard curve and to correct for variations in target sample quantities. Relative copy numbers were calculated for each sample from the standard curve after normalization to HPRT-1 by the instrument software. Primers used: FOXP3_F, 5′- CAGCACATTCCCAGAGTTCC-3′; FOXP3_R,5′-TGAGCGTGGCGTAGGT GAAAG-3′; RORA_F,5′- TCACCAACGGCGAGACTTC-3′; RORA_R,5′-GGCA AACTCCACCACATACTG-3′; RORC_F,5′-CGCTCCAACATCTTCTCC-3′; RO RC_R,5′-CTAACCAGCACCACTTCC-3′; AHR_F,5′-AACAGATGAGGAAGGAA CAGAGC-3′; AHR_R,5′-GAGTGGATGTGGTAGCAGAGTC-3′; AHRR_F,5′- AA GGCTGCTGTTGGAGTC-3′; AHRR_R,5′- TGGATGTAGTCATAAATGTTCTG G-3′; HPRT-1_F,5′-GCTGAGGATTTGGAAAGGGTG-3′; HPRT-1_R,5′-TGAG CACACAGAGGGCTACAATG-3′.

ACCESSION NUMBERS

Microarray data are available from the National Center for Biotechnology Information Gene Expression Omnibus (GEO) under accession number GSE15659.

SUPPLEMENTAL DATA

Supplemental Data include ten figures and two tables and can be found with this article online at http://www.cell.com/immunity/supplemental/S1074-7613(09)00202-7.

ACKNOWLEDGMENTS

This work was supported by grant in aid from the Ministry of Education, Sports, and Culture of Japan. M.M. was successively supported by la Fondation pour la Recherche Médicale and by Japan Society for the Promotion of Science. The study was also in part supported by a grant from the European Union (ATTACK project LHS-CT-2005-018914). We thank the blood donors and the patients who participated in the study, R. Ishii for expertise in cell sorting, M. Kakino for assistance in molecular biology, M. Yoshida for maintaining mice, and S. Teradaira, A. Kishi, M. Hashimoto, S. Maeda, H. Uryu, K. Hirota, C. Badoual, and N. Sakaguchi for technical help and valuable discussion.

Received: December 25, 2008
Revised: February 23, 2009
Accepted: March 26, 2009
Published online: May 21, 2009

REFERENCES

Allan, S.E., Crome, S.Q., Crellin, N.K., Passerini, L., Steiner, T.S., Bacchetta, R., Roncarolo, M.G., and Levings, M.K. (2007). Activation-induced FOXP3 in human T effector cells does not suppress proliferation or cytokine production. Int. Immunol. *19*, 345–354.

Baecher-Allan, C., Brown, J.A., Freeman, G.J., and Hafler, D.A. (2001). CD4+CD25high regulatory cells in human peripheral blood. J. Immunol. *167*, 1245–1253.

Baecher-Allan, C., Wolf, E., and Hafler, D.A. (2006). MHC class II expression identifies functionally distinct human regulatory T cells. J. Immunol. *176*, 4622–4631.

Baron, U., Floess, S., Wieczorek, G., Baumann, K., Grutzkau, A., Dong, J., Thiel, A., Boeld, T.J., Hoffmann, P., Edinger, M., et al. (2007). DNA demethylation in the human FOXP3 locus discriminates regulatory T cells from activated FOXP3(+) conventional T cells. Eur. J. Immunol. *37*, 2378–2389.

Curiel, T.J., Coukos, G., Zou, L., Alvarez, X., Cheng, P., Mottram, P., Evdemon-Hogan, M., Conejo-Garcia, J.R., Zhang, L., Burow, M., et al. (2004). Specific recruitment of regulatory T cells in ovarian carcinoma fosters immune privilege and predicts reduced survival. Nat. Med. *10*, 942–949.

Dieckmann, D., Plottner, H., Berchtold, S., Berger, T., and Schuler, G. (2001). Ex vivo isolation and characterization of CD4(+)CD25(+) T cells with regulatory properties from human blood. J. Exp. Med. *193*, 1303–1310.

Ehrenstein, M.R., Evans, J.G., Singh, A., Moore, S., Warnes, G., Isenberg, D.A., and Mauri, C. (2004). Compromised function of regulatory T cells in rheumatoid arthritis and reversal by anti-TNFalpha therapy. J. Exp. Med. *200*, 277–285.

Floess, S., Freyer, J., Siewert, C., Baron, U., Olek, S., Polansky, J., Schlawe, K., Chang, H.D., Bopp, T., Schmitt, E., et al. (2007). Epigenetic control of the foxp3 locus in regulatory T cells. PLoS Biol. *5*, e38.

Fontenot, J.D., Gavin, M.A., and Rudensky, A.Y. (2003). Foxp3 programs the development and function of CD4+CD25+ regulatory T cells. Nat. Immunol. *4*, 330–336.

Fritzsching, B., Oberle, N., Pauly, E., Geffers, R., Buer, J., Poschl, J., Krammer, P., Linderkamp, O., and Suri-Payer, E. (2006). Naive regulatory T cells: A novel subpopulation defined by resistance toward CD95L-mediated cell death. Blood *108*, 3371–3378.

Gavin, M.A., Torgerson, T.R., Houston, E., DeRoos, P., Ho, W.Y., Stray-Pedersen, A., Ocheltree, E.L., Greenberg, P.D., Ochs, H.D., and Rudensky, A.Y. (2006). Single-cell analysis of normal and FOXP3-mutant human T cells: FOXP3 expression without regulatory T cell development. Proc. Natl. Acad. Sci. USA *103*, 6659–6664.

Hermiston, M.L., Xu, Z., and Weiss, A. (2003). CD45: A critical regulator of signaling thresholds in immune cells. Annu. Rev. Immunol. *21*, 107–137.

Hiramatsu, H., Nishikomori, R., Heike, T., Ito, M., Kobayashi, K., Katamura, K., and Nakahata, T. (2003). Complete reconstitution of human lymphocytes from cord blood CD34+ cells using the NOD/SCID/gammacnull mice model. Blood *102*, 873–880.

Hoffmann, P., Eder, R., Boeld, T.J., Doser, K., Piseshka, B., Andreesen, R., and Edinger, M. (2006). Only the CD45RA+ subpopulation of CD4+CD25high T cells gives rise to homogeneous regulatory T-cell lines upon in vitro expansion. Blood *108*, 4260–4267.

Hori, S., Nomura, T., and Sakaguchi, S. (2003). Control of regulatory T cell development by the transcription factor Foxp3. Science *299*, 1057–1061.

Ito, T., Hanabuchi, S., Wang, Y.H., Park, W.R., Arima, K., Bover, L., Qin, F.X., Gilliet, M., and Liu, Y.J. (2008). Two functional subsets of FOXP3+ regulatory T cells in human thymus and periphery. Immunity *28*, 870–880.

Ivanov, I.I., McKenzie, B.S., Zhou, L., Tadokoro, C.E., Lepelley, A., Lafaille, J.J., Cua, D.J., and Littman, D.R. (2006). The orphan nuclear receptor RORgammat directs the differentiation program of proinflammatory IL-17+ T helper cells. Cell *126*, 1121–1133.

Janson, P.C., Winerdal, M.E., Marits, P., Thorn, M., Ohlsson, R., and Winqvist, O. (2008). FOXP3 promoter demethylation reveals the committed Treg population in humans. PLoS ONE *3*, e1612.

Jonuleit, H., Schmitt, E., Stassen, M., Tuettenberg, A., Knop, J., and Enk, A.H. (2001). Identification and functional characterization of human CD4(+)CD25(+) T cells with regulatory properties isolated from peripheral blood. J. Exp. Med. *193*, 1285–1294.

Khattri, R., Cox, T., Yasayko, S.A., and Ramsdell, F. (2003). An essential role for Scurfin in CD4+CD25+ T regulatory cells. Nat. Immunol. *4*, 337–342.

Kimmig, S., Przybylski, G.K., Schmidt, C.A., Laurisch, K., Mowes, B., Radbruch, A., and Thiel, A. (2002). Two subsets of naive T helper cells with distinct T cell receptor excision circle content in human adult peripheral blood. J. Exp. Med. *195*, 789–794.

Kriegel, M.A., Lohmann, T., Gabler, C., Blank, N., Kalden, J.R., and Lorenz, H.M. (2004). Defective suppressor function of human CD4+ CD25+ regulatory T cells in autoimmune polyglandular syndrome type II. J. Exp. Med. *199*, 1285–1291.

Levings, M.K., Sangregorio, R., and Roncarolo, M.G. (2001). Human cd25(+)cd4(+) t regulatory cells suppress naive and memory T cell proliferation and can be expanded in vitro without loss of function. J. Exp. Med. *193*, 1295–1302.

Liu, W., Putnam, A.L., Xu-Yu, Z., Szot, G.L., Lee, M.R., Zhu, S., Gottlieb, P.A., Kapranov, P., Gingeras, T.R., Fazekas de St Groth, B., et al. (2006). CD127 expression inversely correlates with FoxP3 and suppressive function of human CD4+ T reg cells. J. Exp. Med. *203*, 1701–1711.

Mantel, P.Y., Ouaked, N., Ruckert, B., Karagiannidis, C., Welz, R., Blaser, K., and Schmidt-Weber, C.B. (2006). Molecular mechanisms underlying FOXP3 induction in human T cells. J. Immunol. *176*, 3593–3602.

Miyara, M., Amoura, Z., Parizot, C., Badoual, C., Dorgham, K., Trad, S., Nochy, D., Debre, P., Piette, J.C., and Gorochov, G. (2005). Global natural regulatory T cell depletion in active systemic lupus erythematosus. J. Immunol. *175*, 8392–8400.

Miyara, M., Amoura, Z., Parizot, C., Badoual, C., Dorgham, K., Trad, S., Kambouchner, M., Valeyre, D., Chapelon-Abric, C., Debre, P., et al. (2006). The immune paradox of sarcoidosis and regulatory T cells. J. Exp. Med. *203*, 359–370.

Ng, W.F., Duggan, P.J., Ponchel, F., Matarese, G., Lombardi, G., Edwards, A.D., Isaacs, J.D., and Lechler, R.I. (2001). Human CD4(+)CD25(+) cells: a naturally occurring population of regulatory T cells. Blood *98*, 2736–2744.

Onishi, Y., Fehervari, Z., Yamaguchi, T., and Sakaguchi, S. (2008). Foxp3+ natural regulatory T cells preferentially form aggregates on dendritic cells in vitro and actively inhibit their maturation. Proc. Natl. Acad. Sci. USA *105*, 10113–10118.

Quintana, F.J., Basso, A.S., Iglesias, A.H., Korn, T., Farez, M.F., Bettelli, E., Caccamo, M., Oukka, M., and Weiner, H.L. (2008). Control of T(reg) and T(H)17 cell differentiation by the aryl hydrocarbon receptor. Nature *453*, 65–71.

Roncador, G., Brown, P.J., Maestre, L., Hue, S., Martinez-Torrecuadrada, J.L., Ling, K.L., Pratap, S., Toms, C., Fox, B.C., Cerundolo, V., et al. (2005). Analysis of FOXP3 protein expression in human CD4+CD25+ regulatory T cells at the single-cell level. Eur. J. Immunol. *35*, 1681–1691.

Sakaguchi, S., Sakaguchi, N., Asano, M., Itoh, M., and Toda, M. (1995). Immunologic self-tolerance maintained by activated T cells expressing IL-2 receptor alpha-chains (CD25). Breakdown of a single mechanism of self-tolerance causes various autoimmune diseases. J. Immunol. *155*, 1151–1164.

Sakaguchi, S., Yamaguchi, T., Nomura, T., and Ono, M. (2008). Regulatory T cells and immune tolerance. Cell *133*, 775–787.

Seddiki, N., Santner-Nanan, B., Martinson, J., Zaunders, J., Sasson, S., Landay, A., Solomon, M., Selby, W., Alexander, S.I., Nanan, R., et al. (2006). Expression of interleukin (IL)-2 and IL-7 receptors discriminates between human regulatory and activated T cells. J. Exp. Med. *203*, 1693–1700.

Taams, L.S., Smith, J., Rustin, M.H., Salmon, M., Poulter, L.W., and Akbar, A.N. (2001). Human anergic/suppressive CD4(+)CD25(+) T cells: a highly differentiated and apoptosis-prone population. Eur. J. Immunol. *31*, 1122–1131.

Taflin, C., Miyara, M., Nochy, D., Valeyre, D., Naccache, J.M., Altare, F., Salek-Peyron, P., Badoual, C., Bruneval, P., Haroche, J., et al. (2009). FoxP3+ regulatory T cells suppress early stages of granuloma formation but have little impact on sarcoidosis lesions. Am. J. Pathol. *174*, 497–508.

Tran, D.Q., Ramsey, H., and Shevach, E.M. (2007). Induction of FOXP3 expression in naive human CD4+FOXP3 T cells by T-cell receptor stimulation is transforming growth factor-{beta} dependent but does not confer a regulatory phenotype. Blood *110*, 2983–2990.

Valmori, D., Merlo, A., Souleimanian, N.E., Hesdorffer, C.S., and Ayyoub, M. (2005). A peripheral circulating compartment of natural naive CD4 Tregs. J. Clin. Invest. *115*, 1953–1962.

Veldhoen, M., Hirota, K., Westendorf, A.M., Buer, J., Dumoutier, L., Renauld, J.C., and Stockinger, B. (2008). The aryl hydrocarbon receptor links T(H)17-cell-mediated autoimmunity to environmental toxins. Nature *453*, 106–109.

Viglietta, V., Baecher-Allan, C., Weiner, H.L., and Hafler, D.A. (2004). Loss of functional suppression by CD4+CD25+ regulatory T cells in patients with multiple sclerosis. J. Exp. Med. *199*, 971–979.

Vrisekoop, N., den Braber, I., de Boer, A.B., Ruiter, A.F., Ackermans, M.T., van der Crabben, S.N., Schrijver, E.H., Spierenburg, G., Sauerwein, H.P., Hazenberg, M.D., et al. (2008). Sparse production but preferential incorporation of recently produced naive T cells in the human peripheral pool. Proc. Natl. Acad. Sci. USA *105*, 6115–6120.

Vukmanovic-Stejic, M., Zhang, Y., Cook, J.E., Fletcher, J.M., McQuaid, A., Masters, J.E., Rustin, M.H., Taams, L.S., Beverley, P.C., Macallan, D.C., and

Akbar, A.N. (2006). Human CD4+ CD25hi Foxp3+ regulatory T cells are derived by rapid turnover of memory populations in vivo. J. Clin. Invest. *116*, 2423–2433.

Wang, J., Ioan-Facsinay, A., van der Voort, E.I., Huizinga, T.W., and Toes, R.E. (2007). Transient expression of FOXP3 in human activated nonregulatory CD4+ T cells. Eur. J. Immunol. *37*, 129–138.

Wing, K., Onishi, Y., Prieto-Martin, P., Yamaguchi, T., Miyara, M., Fehervari, Z., Nomura, T., and Sakaguchi, S. (2008). CTLA-4 control over Foxp3+ regulatory T cell function. Science *322*, 271–275.

Yagi, H., Nomura, T., Nakamura, K., Yamazaki, S., Kitawaki, T., Hori, S., Maeda, M., Onodera, M., Uchiyama, T., Fujii, S., and Sakaguchi, S. (2004). Crucial role of FOXP3 in the development and function of human CD25+CD4+ regulatory T cells. Int. Immunol. *16*, 1643–1656.

Yang, X.O., Nurieva, R., Martinez, G.J., Kang, H.S., Chung, Y., Pappu, B.P., Shah, B., Chang, S.H., Schluns, K.S., Watowich, S.S., et al. (2008a). Molecular antagonism and plasticity of regulatory and inflammatory T cell programs. Immunity *29*, 44–56.

Yang, X.O., Pappu, B.P., Nurieva, R., Akimzhanov, A., Kang, H.S., Chung, Y., Ma, L., Shah, B., Panopoulos, A.D., Schluns, K.S., et al. (2008b). T helper 17 lineage differentiation is programmed by orphan nuclear receptors ROR alpha and ROR gamma. Immunity *28*, 29–39.

Zhou, L., Lopes, J.E., Chong, M.M., Ivanov, I.I., Min, R., Victora, G.D., Shen, Y., Du, J., Rubtsov, Y.P., Rudensky, A.Y., et al. (2008). TGF-beta-induced Foxp3 inhibits T(H)17 cell differentiation by antagonizing RORgammat function. Nature *453*, 236–240.

Zorn, E., Nelson, E.A., Mohseni, M., Porcheray, F., Kim, H., Litsa, D., Bellucci, R., Raderschall, E., Canning, C., Soiffer, R.J., et al. (2006). IL-2 regulates FOXP3 expression in human CD4+CD25+ regulatory T cells through a STAT-dependent mechanism and induces the expansion of these cells in vivo. Blood *108*, 1571–1579.

Impaired CD4 and CD8 Effector Function and Decreased Memory T Cell Populations in ICOS-Deficient Patients

Naomi Takahashi,* Kenji Matsumoto,† Hirohisa Saito,† Toshihiro Nanki,‡ Nobuyuki Miyasaka,‡ Tetsuji Kobata,§ Miyuki Azuma,¶ Sang-Kyou Lee,‖ Shuki Mizutani,* and Tomohiro Morio[1]*

Interaction of ICOS with its ligand is essential for germinal center formation, T cell immune responses, and development of autoimmune diseases. Human ICOS deficiency has been identified worldwide in nine patients with identical ICOS mutations. In vitro studies of the patients to date have shown only mild T cell defect. In this study, we report an in-depth analysis of T cell function in two siblings with novel ICOS deficiency. The brother displayed mild skin infections and impaired Ig class switching, whereas the sister had more severe symptoms, including immunodeficiency, rheumatoid arthritis, inflammatory bowel disease, interstitial pneumonitis, and psoriasis. Despite normal CD3/CD28-induced proliferation and IL-2 production in vitro, peripheral blood T cells in both patients showed a decreased percentage of CD4 central and effector memory T cells and impaired production of Th1, Th2, and Th17 cytokines upon CD3/CD28 costimulation or PMA/ionophore stimulation. The defective polarization into effector cells was associated with impaired induction of T-bet, GATA3, MAF, and retinoic acid-related orphan nuclear hormone receptor (RORC). Reduced CTLA-4$^+$CD45RO$^+$FoxP3$^+$ regulatory T cells and diminished induction of inhibitory cell surface molecules, including CTLA-4, were also observed in the patients. T cell defect was not restricted to CD4 T cells because reduced memory T cells and impaired IFN-γ production were also noted in CD8 T cells. Further analysis of the patients demonstrated increased induction of receptor activator of NF-κB ligand (RANKL), lack of IFN-γ response, and loss of Itch expression upon activation in the female patient, who had autoimmunity. Our study suggests that extensive T cell dysfunction, decreased memory T cell compartment, and imbalance between effector and regulatory cells in ICOS-deficient patients may underlie their immunodeficiency and/or autoimmunity. *The Journal of Immunology,* **2009, 182: 5515–5527.**

Members of the CD28 family play an important role in the regulation of T cell immune responses (1, 2). Expression of these molecules and their ligands is tightly regulated to deliver either costimulatory or inhibitory signals (2–5), and their uncoordinated regulation leads to the development of immunological disorders (6–8).

ICOS (CD278) is a costimulatory member of the CD28 family, and its expression is induced in CD4 T cells upon activation (9–11). The ICOS signal is induced by interaction with its partner, the ICOS ligand (ICOS-L[2]; CD275), a molecule highly expressed on B cells and dendritic cells and weakly on T cells and nonlymphoid cells (1, 12). Signaling through ICOS enhances T cell proliferation, secretion of cytokines, and up-regulation of cell surface molecules (11, 13, 14).

Previous research has showed that the ICOS-ICOS-L interaction is important for productive T-B cell coactivation, CD40-mediated Ig class switch recombination, and development of Th2 immune responses (1, 15–17). Induction of the Th1 cytokine IFN-γ is relatively unaffected and in some studies augmented; other studies have documented the importance of ICOS in Th1 responses (15, 16, 18–21). Accumulating evidence indicates that ICOS also regulates the generation of Th17 cells, differentiation of FoxP3$^+$ regulatory T cells (Tregs), and homeostatic survival of invariant NKT (iNKT) cells (22–24).

Although earlier investigations of ICOS-null mice revealed normal numbers of naive/memory T cells and normal primary clonal expansion and survival of memory T cells, more recent investigation has demonstrated lower numbers of effector memory T cells (TEMs) in ICOS$^{-/-}$ mice in the steady state (23). Seemingly contradictory results have been reported on the requirement of ICOS for T cell differentiation and function.

Most studies have depicted ICOS as a costimulator. Indeed, the blockade of the ICOS-ICOS-L interaction abrogates the development of murine models of autoimmune diseases, as follows: rheumatoid arthritis (RA), inflammatory bowel disease (IBD), myasthenia gravis, type I diabetes mellitus, experimental myositis, autoimmune carditis, and graft-vs-host disease (25–30).

Previously, human ICOS deficiency has been reported in nine patients from four families (31–33). Importantly, the same homologous genetic deletion of exons 2 and 3 was identified in all patients, indicating a founder effect in all four families. Analysis of these patients revealed reduced numbers of memory B cells and pan-hypoimmunoglobulinemia, but no impairment in the secretion of TNF-α, IFN-γ, IL-2, IL-4, IL-10, or IL-13. Normal surface

*Department of Pediatrics and Developmental Biology, Graduate School of Medical and Dental Sciences, Tokyo Medical and Dental University, Tokyo, Japan; †Department of Allergy and Immunology, National Research Institute for Child Health and Development, Tokyo, Japan; ‡Department of Medicine and Rheumatology, Graduate School of Medical and Dental Sciences, Tokyo Medical and Dental University, Tokyo, Japan; §Department of Immunology, Dokkyo Medical University, Tochigi, Japan; ¶Department of Molecular Immunology, Graduate School of Medical and Dental Sciences, Tokyo Medical and Dental University, Tokyo, Japan; and ‖Department of Biotechnology, Yonsei University, Seoul, Korea

Received for publication October 6, 2008. Accepted for publication February 24, 2009.

The costs of publication of this article were defrayed in part by the payment of page charges. This article must therefore be hereby marked *advertisement* in accordance with 18 U.S.C. Section 1734 solely to indicate this fact.

[1] Address correspondence and reprint requests to Dr. Tomohiro Morio, Tokyo Medical and Dental University Graduate School of Medicine, 1-5-45 Yushima, Bunkyo-Ku, Tokyo 113-8519, Japan. E-mail address: tmorio.ped@tmd.ac.jp

[2] Abbreviations used in this paper: ICOS-L, ICOS ligand; IBD, inflammatory bowel disease; IP, interstitial pneumonitis; RA, rheumatoid arthritis; RE, relative expression; TCM, central memory T cell; TEM, effector memory T cell; Treg, regulatory T cell; BTLA, B and T lymphocyte attenuator; EOMES, eomesodermin; PD-1, programmed death-1; RANKL, receptor activator of NF-κB ligand; RORC, retinoic acid-related orphan nuclear hormone receptor.

www.jimmunol.org/cgi/doi/10.4049/jimmunol.0803256

expression of CD69, CD40L (CD154), CD25, and OX40 (CD134) was observed on their T cells following stimulation (31). A later study provided evidence of defects in IL-10 and IL-17 production (33); however, no major impairment of T cell function was demonstrated. Autoimmunity, manifested as autoantibody-mediated neutropenia, was observed in only one patient (33). Although there have been reports on the effects of ICOS on CD8 responses in mice (34, 35), impact of ICOS on CD8 T cells is not yet completely understood.

In this study, we describe the case of two siblings having ICOS deficiency with a novel mutation in the ICOS gene. Although both patients displayed varing degrees of immunodeficiency, only the sister showed a wide range of autoimmune diseases, including RA, IBD, interstitial pneumonitis (IP), and psoriasis.

In this study, we focused on the T cell immune function of these ICOS-deficient patients. Detailed analysis demonstrated a reduction in memory T cells and a major subtype of Tregs; impaired polarization into Th1, Th2, and Th17; and defective induction of CTLA-4 molecules and other surface inhibitory receptors.

We further assessed activation-induced T cell proliferation and apoptosis, induction of costimulatory receptor molecules, and expression of master regulators for effector T cell subsets, and explored the mechanisms of T cell defect and autoimmunity in these patients using quantitative mRNA analysis.

Materials and Methods

Patients and controls

Patients were diagnosed with common variable immunodeficiency, according to the European Society for Immunodeficiencies criteria (www.esid.org). Twelve healthy volunteers (6 male, 6 female) aged between 26 and 48 years were recruited. The study was approved by the institutional ethical committee of Tokyo Medical and Dental University, and written informed consent was obtained from the patients, the elder sister and mother of the patients, and healthy controls.

Sequencing and RT-PCR of ICOS

Genomic DNA was extracted from peripheral blood using a DNA blood mini kit (Qiagen), according to the manufacturer's instructions. The coding sequences of the five exons and the adjacent intron-exon boundaries of the ICOS gene were amplified with specific primers (sequences are available upon request) from genomic DNA on the basis of ICOS sequences obtained from GenBank database (accession numbers AC103880, AC009965, and AB023135). All PCR products were sequenced using BigDye terminator v3.1 and an ABI Prism 3130 Genetic Analyzer (Applied Biosystems); the sequence data were then analyzed using DNASIS software (Hitachi Software). Total RNA was isolated from stimulated PBMCs using an RNeasy mini kit (Qiagen) and reverse transcribed into cDNA using a Superscript III first-strand synthesis system for RT-PCR (Invitrogen). PCR products were separated by agarose gel electrophoresis.

Monoclonal Abs

We used the following FITC-, PE-, PE Texas Red (ECD)-, or PE cyanin 5.1 (PC5)-conjugated Abs: FoxP3 (236A/E7) from Abcam; IgG1 isotype controls, CD3 FITC, CD3 PE (SK7), CD4 PE (SK3), CD8 FITC, CD8 PE (SK1), CD25 FITC (M-A251), IL-4 PE (3010.211), IFN-γ PE (25723.11), 4-1BB PE (4B4-1), OX40 PE (ACT35), and IL-10 PE (JES3-10F1) from BD Pharmingen; CD3 FITC (UCHT1), CD4 PC5 (13B8.2), CD8 ECD (SFCI21Thy2D3), CD8 FITC (B9.11), CD19 ECD, CD19 PE (J4.119), CD20 FITC (B9E9), CD25 PC5 (B1.49.1), CD28 FITC, CD28 purified (CD28.2), CD45RA FITC (ALB11 and 2H4), CD45RO PE, ECD (UCHL1), CD62L ECD (DREG56), CD69 PE (TP1.55.3), CTLA4 PE (BNI3), streptavidin FITC, streptavidin PC5, and TCR Vβ Repertoire kit from Beckman Coulter (CA); CD27 PE (M-T271) and IgD from Dako-Cytomation; CD45RO PE (UCHL1), IL-17 FITC (eBio64DEC17), B and T lymphocyte attenuator (BTLA) PE (MIH26), programmed death-1 (PD-1) FITC (MIH4), ICOS-L, ICOSL biotin (MIH12), and ICOS FITC (ISA-3) from eBioscience; receptor activator of NF-κB (RANK) PE (9A725) from Imgenex; CD25 PE (4E3) from Miltenyi Biotec; Alexa Fluor 488 goat anti-mouse IgG Ab from Molecular Probes; CCR7 FITC (150503) from eBioscience; and CD3 purified (OKT3) from Janssen Pharmaceutical.

Cell separation and stimulation

PBMCs were isolated from heparinized blood using Lymphoprep (Axis-Shield), as described previously (36). CD4 T cells were negatively selected from the PBMCs using a StemSep device (StemCell Technologies). Thus, the purity of the collected CD4 T cell population was generally >95%. CD8 T cells were prepared with the same technique yielding >90% pure CD8 T cell population. Separated cells were resuspended in RPMI 1640 (WAKO) supplemented with 10% heat-inactivated FBS (Gemini Biological Products), and incubated at 10^6 cells/ml in 24-well plates (Greiner Bioscience) with or without stimulants. For stimulation, we used anti-CD28 mAb (at 1 μg/ml) with plate-bound anti-CD3 mAb or 50 ng/ml PMA (Sigma-Aldrich) plus 1 μg/ml ionomycin (Sigma-Aldrich). The cells were incubated in the medium at 37°C in 5% CO_2 for the indicated time periods. IL-2 (Lymphotec) was used at 700 IU/ml with plate-bound anti-CD3 when assessing ICOS expression.

Flow cytometric analysis

PBMCs, CD4 T cells, or CD8 T cells were stained with the indicated Abs and were analyzed using a FACSCalibur flow cytometer and CellQuest software (BD Biosciences) or an EPICS XL flow cytometer and EXPO32 software (Beckman Coulter), as described previously (37). For intracellular cytokine detection, PBMCs were stimulated with PMA and ionomycin in the presence of GolgiPlug (BD Pharmingen) or brefeldin A (eBioscience) for 5–8 h at 37°C in 5% CO_2. After stimulation, the cells were fixed and permeabilized using a Cytofix/Cytoperm Plus fixation/permeabilization kit (BD Pharmingen). The same permeabilization technique was used to detect CTLA-4 expression. A CellTrace CFSE cell proliferation kit (Molecular Probes) was used for the CFSE assay, and an annexin V FITC/7-AAD kit (Beckman Coulter) for the apoptosis assay.

Cytokine production assay

Negatively selected CD4 T cells or CD8 T cells were incubated with or without stimulants (plate-bound anti-CD3 mAb and anti-CD28 mAb or 50 ng/ml PMA, and 200 nM ionomycin). The supernatants were collected after 24 h and analyzed using ELISA for IL-17, IL-12p40, IL-22, and TGF-β1 (R&D Systems); IL-21 (eBioscience); and human Th1/Th2 cytokines (IFN-γ, IL-2, IL-4, IL-5, IL-6, IL-10, TNF-α, and TNF-β) using a FlowCytomix kit (Bender MedSystems), according to the manufacturer's instructions. All assays were performed in duplicate.

Real-time quantitative PCR

Total RNA was extracted using an RNeasy mini kit with DNase (Qiagen) and reverse transcribed using random hexamer primers and Superscript III reverse transcriptase (Invitrogen). Real-time quantitative PCR was performed using a 7300 Real-Time PCR system (Applied Biosystems) using an assay-on-demand Taqman probe and primers (Hs00174383 for *IL17A*, Hs00243522 for *RANKL*, Hs00203958 for *FOXP3*, Hs00226053 for *RNF128*, Hs00909784 for *CBLB*, Hs00395208 for *ITCH*, Hs00172872 for *EOMES*, Hs00193519 for *MAF*, Hs00231122 for *GATA3*, Hs00894392 for *TBX21*, Hs01076112 for *RORC*, Hs99999901 for *18S*, and Hs99999905 for *GAPDH*), according to the manufacturer's instructions. Relative expression levels of these genes were normalized according to *GAPDH* or *18S rRNA* expression, using a standard curve method as described by the manufacturer. All samples and standards were tested in duplicate.

Oligonucleotide microarray assay

Oligonucleotide microarray assay was conducted with total RNA extracted from a total of 1–3 × 10^6 CD4 T cells stimulated in anti-CD3-coated plates in the presence of anti-CD28 mAb or from unstimulated CD4 T cells, as described previously (38). Data analysis, selection of significant signals, and comparison of the data from multiple samples were conducted, as previously described (38). The results have been deposited in the Gene Expression Omnibus at http://www.ncbi.nlm.nih.gov/geo/(accession number GSE12875).

Results

Clinical course of patients and diagnosis of ICOS deficiency

The sister, hereafter designated patient 1, was born in 1967. In her infancy, she had episodes of prolonged viral infection. In 2001, when she developed a pulmonary abscess following appendectomy, she was diagnosed with common variable immunodeficiency according to the European Society for Immunodeficiencies criteria (at the age of 34), and i.v. Ig treatment was started to

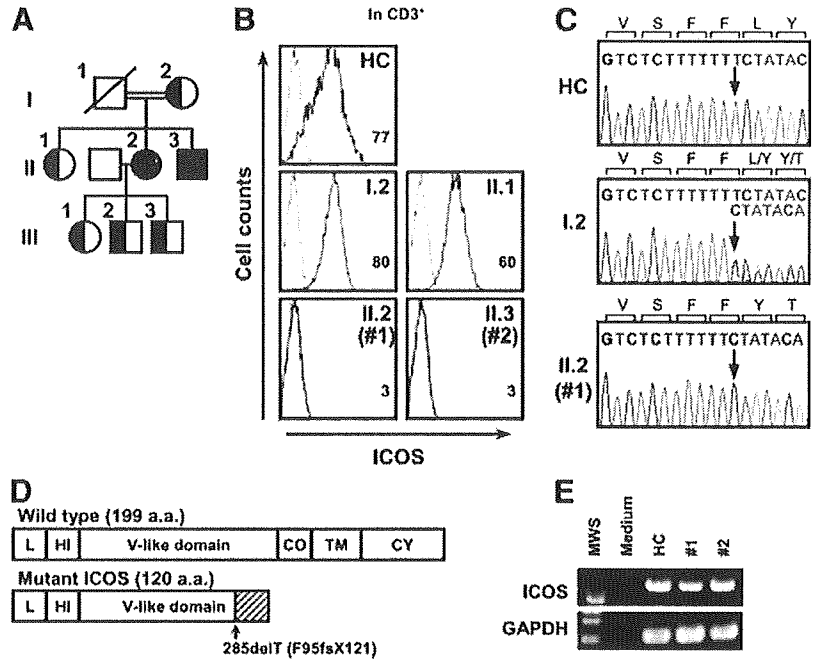

FIGURE 1. Diagnosis of ICOS deficiency. *A*, Pedigree of the ICOS deficiency patients. Filled symbols represent affected family members (II.2, patient 1; II.3, patient 2). The patients were products of a consanguineous marriage. *B*, Expression of ICOS. PBMCs from patients 1 and 2, their mother (I.2), elder sister (II.1), and a healthy control (HC) were cultured on an anti-CD3 mAb-coated plate in the presence of IL-2 and stained with anti-ICOS mAb (solid line) or control mAb (dotted line). The graphs are gated on CD3 T cells. Mean fluorescence intensity of ICOS is shown in each graph. *C*, Partial sequences of exon 2 of *ICOS* from HC, the mother of the patients, and patient 1. The elder sister of the patients had a heterozygous mutation that was detected in the mother, and the brother (patient 2) had a homozygous mutation at codon 285. *D*, Schematic figure showing the wild-type 199-aa ICOS protein and putative 120-aa mutant ICOS protein obtained from the patients. The shaded area represents the mutant proteins generated by induction of a frameshift at codon 285. L, L region; HI, hydrophilic region; CO, connecting region; TM, transmembrane region; CY, cytoplasmic region. *E*, RT-PCR analysis for *ICOS* mRNA. *ICOS* mRNA (1–597) from anti-CD3/IL-2-stimulated PBMCs from patient 1 (#1) and patient 2 (#2), and HC was amplified by RT-PCR with specific primers. The PCR product was analyzed by agarose gel electrophoresis. MWS, m.w. standard.

maintain the trough IgG level of >4 g/L. In the following years, she developed psoriasis-like cutaneous lesions and arthritis in multiple joints, including bilateral shoulder, wrist, knee, metacarpophalangeal, proximal interphalangeal, and metatarsophalangeal joints. RA was diagnosed on the basis of the findings of proliferative synovitis of multiple finger and toe joints with erosive changes on x-ray examination. Psoriatic arthritis was ruled out based on the joints affected and the x-ray findings. In 2003, she developed abdominal colic, diarrhea, and IP, and had a constantly elevated serum CRP level. Diagnosis of IBD was made upon biopsy of the colon, and both IBD and IP were controlled by prednisolone. She was referred to our hospital in 2006. Methotrexate at 8 mg/week significantly improved not only the articular signs and symptoms of RA, but also the psoriatic skin changes and IBD. The dose of prednisolone was successfully tapered from 15 to 8 mg/day. Since then, she has been on regular Ig supplementation every 2 wk.

The pedigree of the patient is shown in Fig. 1*A*. The patient had two siblings: her sister was healthy with no immunological abnormalities, whereas her younger brother (hereafter designated patient 2) developed occasional skin abscesses and mild psoriasis-like cutaneous lesions, and had slightly low levels of IgG (611 mg/dL) when examined at the age of 35. The serum IgG level stays at the same level to date; and he is not yet on Ig supplementation.

A summary of the immunological data of patients 1 and 2, the elder sister, and ICOS deficiency patients reported to date (33) is given in Table I. Patient 1 had a slightly reduced B cell count, whereas patient 2 had a normal B cell count. In both siblings, however, $CD27^+IgD^-$-switched memory B cells were virtually absent in the peripheral blood samples (Table I). The serum samples contained no detectable specific IgG Abs against measles, mumps, or rubella viruses despite a previous record of vaccine inoculation (data not shown). The immunological parameters of patient 2 are unique in that he showed elevated serum IgM (456 mg/dL). The T cells of the patients displayed abundant expression of CD69 and HLA-DR when stimulated via TCRs in the presence of exogenous IL-2 (data not shown), but lacked surface ICOS expression (Fig. 1*B*). Activated T cells from the mother (I.2) and elder sister (II.1) displayed normal ICOS induction.

Sequencing of the ICOS gene revealed the homozygous deletion of T at codon 285, which caused a frameshift in the coding region of ICOS and introduced a premature stop codon at aa 121 (F95fsX121) in the patients (Fig. 1, *C* and *D*).

Sequencing analysis of the *ICOS* gene in the elder sister and mother demonstrated a heterozygous mutation (Fig. 1*C*). RT-PCR of *ICOS* mRNA with specific primers amplifying the entire coding region of the *ICOS* gene (1–597) demonstrated the presence of an *ICOS* transcript, suggesting the absence of nonsense-mediated RNA decay (Fig. 1*E*).

Decreased memory T cells in ICOS-deficient patients

A previous report on human ICOS-deficient patients showed a normal distribution of naive, memory, and effector T cells (31, 33, 39). However, as seen in the representative FACS plots in Fig. 2*A*, we observed a substantial reduction in $CD4^+CD45RO^+$ memory cells in the patients compared with age- and gender-matched controls (12.1 and 6.6% for patients 1 and 2, respectively, and 24.5

Table I. *Summary of immunological data*[a]

	Patient 1	Patient 2	Previously Reported ICOS-Deficient Patients (range)	II.1 (hetero)	Normal Range
Lymphocytes (/mm^3)	1,400 ± 200	1,900 ± 200	353–4,153	1,400	1,200–2,800
Immunophenotype of PBMCs (%)					
CD3	80.5 ± 5.0	72.4 ± 2.0	70.4–95.6	71.7	58–84
CD4	59.5 ± 5.0	55.6 ± 3.0	23.1–59.2	50.5	25–58
CD8	24.1 ± 4.0	19.1 ± 3.0	16.6–64.0	22.5	18–46
CD16	7.8 ± 0.2	11.2 ± 2.0	–	14.5	6–25
CD19	2.1 ± 0.6	4.8 ± 0.5	0.6–21.2	9.7	3–20
CD19$^+$CD27$^+$(%Bc)	0.2	0.8	2.0–12.6	11.4	8–35
CD19$^+$CD27$^+$IgD$^-$(%Bc)	0	0.4	0.0–1.3	8.6	7–32
Blastogenesis (cpm)					
PHA	56,100	45,600	78,900–95,700	–	20,500–56,800
Con A	45,300	32,500	–	–	20,300–65,700
Igs					
IgG (mg/dL)	315	611		1,025	900–1,600
IgG1	–	322	2.8–181	–	
IgG2	–	365	10–71.7	–	
IgG3	–	19.5	4–44.9	–	
IgG4	–	< 3.0	0–7	–	
IgM (mg/dL)	56	456	20–180	143	40–250
IgA (mg/dL)	46	103	6–58	137	100–250
IgE (IU/L)	<5	<5	17.5–38	ND	<173

[a] Immunological data of patients 1 and 2 are summarized. Lymphocyte counts and immunophenotyping of PBMCs were performed on more than three separate occasions; these are expressed as mean ± SD. Ig levels shown are those obtained at diagnosis (before Ig supplementation). Data from previous reported ICOS deficiency (33) and data from the elder sister of the patients are also shown. %Bc: % in B cells.

and 28.9% for controls 1 and 2, respectively). This reduction was seemingly counterbalanced by an increased frequency of naive T cells.

Gated CD4 memory T cells from PBMCs were further analyzed for CCR7 and CD62L expression to define CCR7$^+$-CD62L$^+$CD45RO$^+$ central memory T cells (TCMs) and

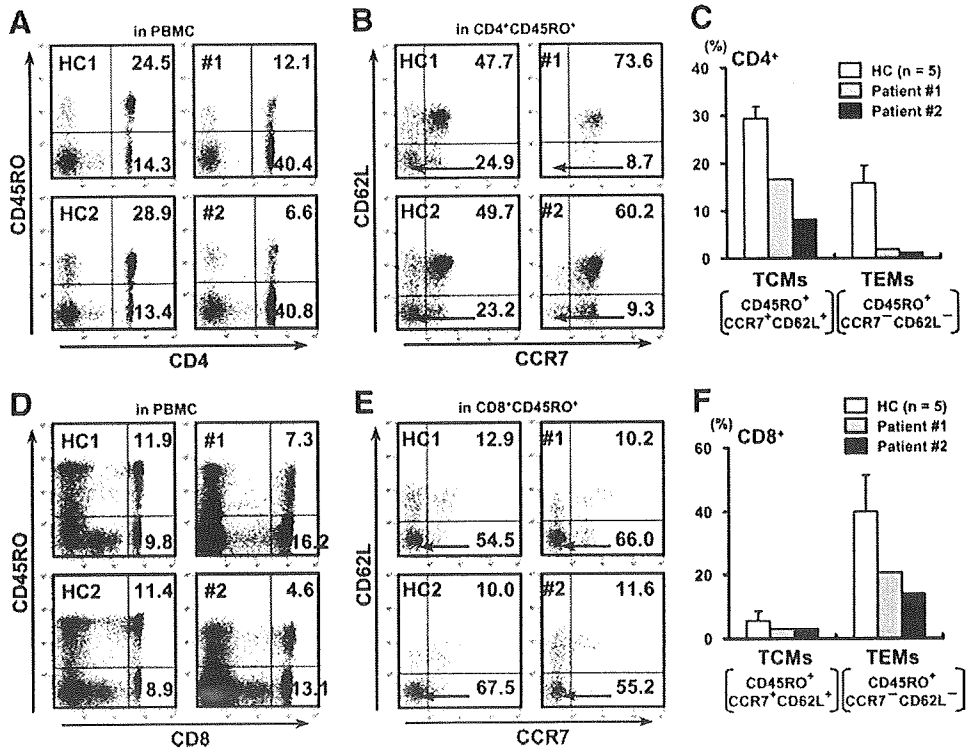

FIGURE 2. Decrease in memory T cells in ICOS-deficient patients. PBMCs from healthy controls (HC) and ICOS-deficient patients (1 and 2) were analyzed for the frequency of memory T cells. PBMCs were stained with Abs to CD4 or CD8, CD45RO, CCR7, and CD62L to assess memory T cell subsets (*A–F*). *A* and *D*, Representative CD4/CD45RO (*A*) and CD8/CD45RO (*D*) dot blots. Values shown in *upper* and *lower right quadrants* indicate percentages of the cells among total PBMCs. *B* and *E*, TCMs (CCR7$^+$CD62L$^+$) and TEMs (CCR7$^-$CD62L$^-$) in the memory CD4 T cell fraction (*B*) and in the memory CD8 T cell fraction (*E*). Values indicate frequencies of TCMs and TEMs in the CD4$^+$CD45RO$^+$ population or in the CD8$^+$CD45RO$^+$ population. Representative FACS analyses for healthy controls (HC) and patients are shown. *C* and *F*, Summary of percentages of TCMs and TEMs among CD4 T cells (*C*) and CD8 T cells (*F*). A □ with error bar represents the mean ± SD values of the indicated subsets from five healthy controls. Mean percentage for the respective subsets from two independent experiments is shown for the patients.

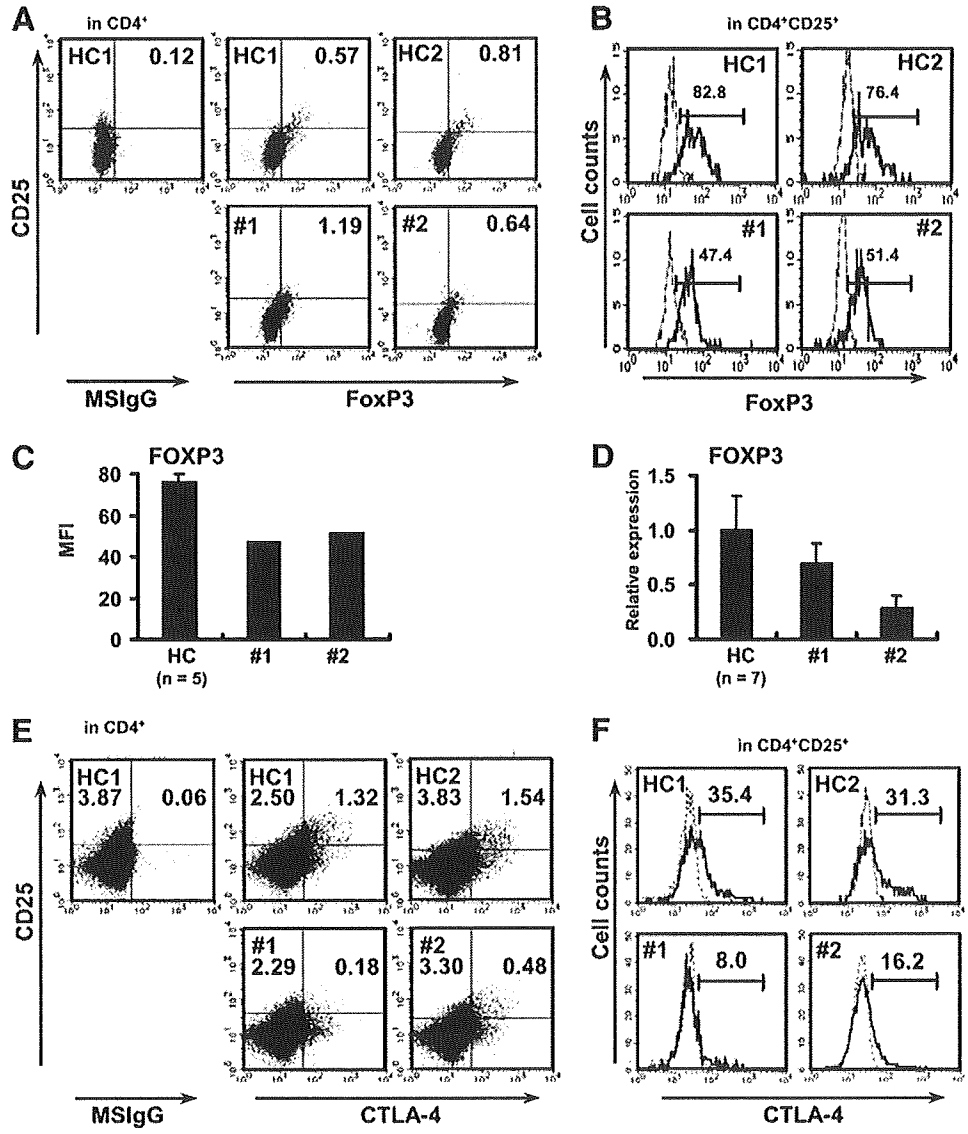

FIGURE 3. Decrease in CTLA-4$^+$ Treg subset in ICOS-deficient patients. *A*, Flow cytometric analysis of intracellular Foxp3 expression in CD4$^+$CD25$^+$ T cells. Numbers in dot plots are percentages of CD25$^+$-Foxp3$^+$ cells among CD4$^+$ T cells. *B*, Mean fluorescence intensity (MFI) of FoxP3 in CD4$^+$CD25$^+$ cells. FoxP3 expression in CD4$^+$CD25$^+$ cells is shown as a contour plot. MFI of FoxP3 is shown in the *upper right quadrant*. *C*, Summary of MFI of FoxP3 in CD4$^+$CD25$^+$ cells. *D*, Quantitative real-time PCR analysis for FoxP3 gene expression. mRNA expression levels in purified CD4 T cells were calculated with 18S rRNA as a reference, and the relative expression in healthy controls (HC) was adjusted to 1.0. Error bar indicates SD for HC and SEM for patients 1 and 2. *E* and *F*, Expression of CTLA-4 Ag in CD4$^+$CD25$^+$ T cells. Numbers indicate frequencies of CTLA-4$^+$ and CTLA-4$^-$ Treg subsets among CD4$^+$ T cells. PBMCs from five HC were analyzed by FACS. FACS analysis was performed three times for the patients. Representative dot plots (*E*) and contour plots (*F*) are shown. MFI of CTLA-4 in CD4$^+$CD25$^+$ Treg cells is indicated in the plots (*F*).

CCR7$^-$CD62L$^-$CD45RO$^+$ TEMs (40). The analysis showed that compared with controls, the patients had 2- to 5-fold fewer TCMs. The reduction in TEMs was more pronounced, with more than 6-fold fewer TEMs in the patients (Fig. 2, *B* and *C*).

A decrease in memory T cells was also observed in CD8 T cells. We observed a reduction in both TCMs and TEMs in patients compared with control subjects (n = 5) (Fig. 2, *D–F*).

Decreased Tregs in ICOS-deficient patients

Most Tregs express ICOS, and ICOS^{high+} Tregs preferentially produce IL-10 (41). In addition, recent studies have demonstrated the importance of ICOS in proliferation and maintenance of the pool size of FoxP3$^+$ Tregs (41). We therefore investigated the frequency of Treg cells in the two patients by staining their PBMCs for CD4, CD25, and intracellular FoxP3. Contrary to our predictions, the patients had a normal proportion of CD4$^+$CD25$^+$FoxP3$^+$ Tregs (Fig. 3*A*). However, we noted that the expression level of FoxP3, as reflected by the mean fluorescence intensity, was diminished in both patients (Fig. 3, *B* and *C*). To ascertain the low FoxP3 expression obtained in the FACS analysis, we evaluated the level of FoxP3 mRNA in a real-time PCR assay. This showed a marked reduction in FoxP3 expression in patient 2 and a slight decrease in patient 1 compared with the normal subjects (n = 7) (Fig. 3*D*).

Recent studies have shown that human CD4$^+$CD25$^+$FoxP3$^+$ Tregs comprise two subsets, as follows: IL-10-producing ICOS$^+$CD45RO$^+$CTLA-4$^+$ Tregs and TGF-β-producing ICOS$^-$CD45RA$^+$CTLA-4^{dull+} Tregs (42). This prompted us to examine CTLA-4 and CD45RO expression in the Tregs of ICOS-deficient patients. Fig. 3, *E* and *F*, demonstrates that most CD4$^+$CD25$^+$ Tregs in these patients were of the CTLA-4^{dull+} or CTLA-4$^-$ subpopulation and expressed CD45RA (data not shown), indicating that the CTLA-4$^+$ subset of Tregs that potentially produces IL-10 was severely decreased.

Defective induction of inhibitory molecules in ICOS-deficient patients

ICOS-null mice showed defective CD40-mediated Ig class switching because of lack of effective CD40L (CD154) up-regulation (15, 16). In contrast, induction of CD40L was normal in the previously reported cases of human ICOS deficiency (33). Up-regulation of 4-1BB (CD137), BTLA (CD272), and CTLA-4 (CD152) was normal in ICOS knockout mice (23), as was that of OX40 (CD134) and CTLA-4 in patients with ICOS deficiency in a previous study (31).

We estimated the expression of these costimulatory and inhibitory receptors on ICOS$^{-/-}$ T cells. PBMCs from controls and patients were stimulated with PMA/ionophore (data not shown) or anti-CD3/

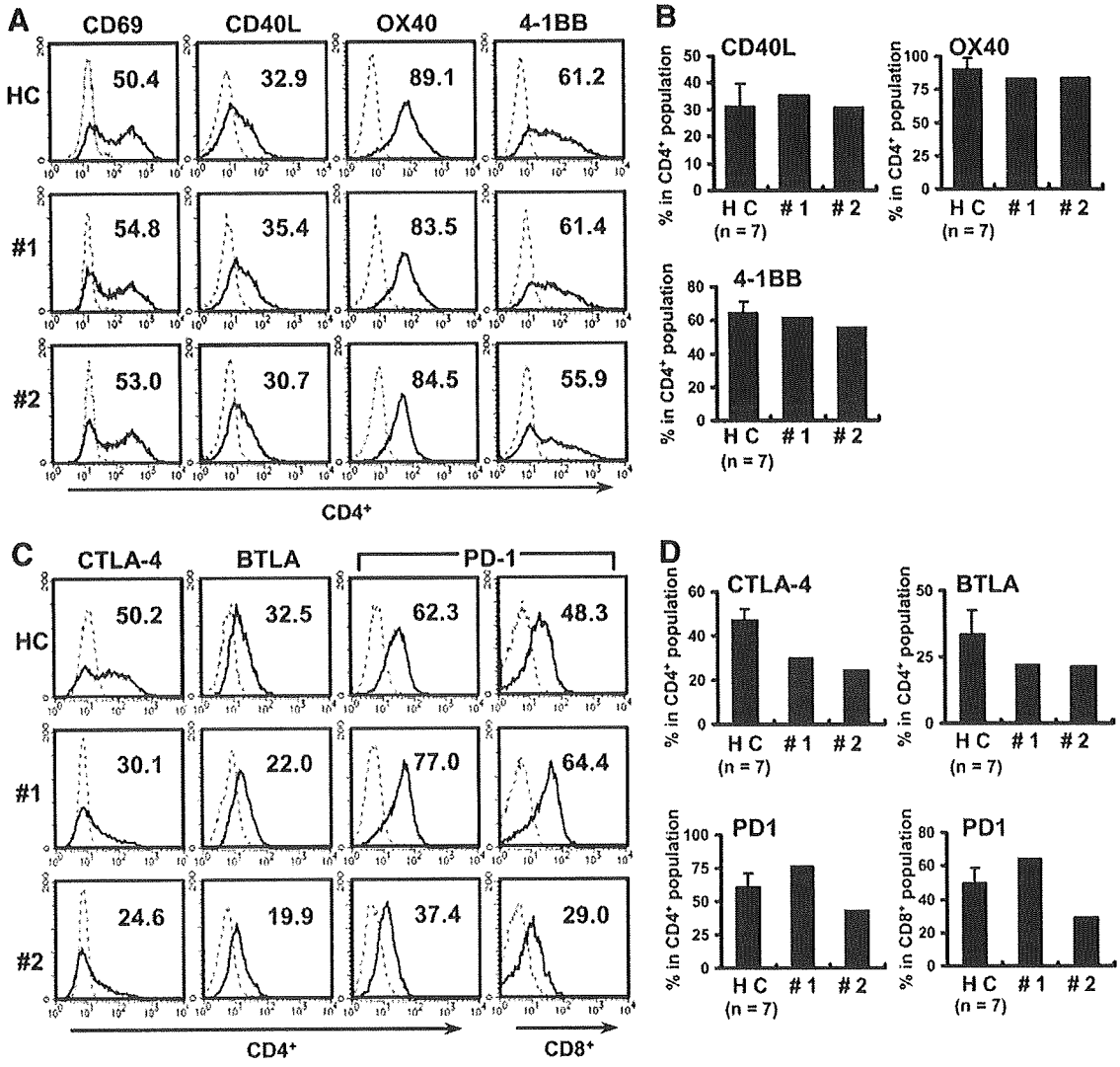

FIGURE 4. Induction of costimulatory and inhibitory molecules in ICOS-deficient patients. *A*, Induced expression of CD40L, OX40, and 4-1BB. PBMCs from healthy controls (HC) and ICOS-deficient patients (#1 and #2) were stimulated with plate-bound anti-CD3 mAb and anti-CD28 mAb for 48 h and analyzed for CD40L, OX40, and 4-1BB expression by FACS. CD69 expression was monitored as an indicator of cell activation. Numbers indicate percentages of the cell population positive for the indicated Ags among CD4 T cells. A contour plot from one representative control of seven HC is shown for each subset. A dotted line indicates a control staining with isotype-matched Ab. *B*, Summary of frequencies of CD40L, OX40, and 4-1BB in CD4 T cells stimulated as in *A* from HC (n = 7) and patients 1 and 2. FACS analysis was performed twice for the patients, and average percentages were plotted. Error bar indicates SD. *C*, Induction of CTLA-4, BTLA, and PD-1. PBMCs were stimulated with plate-bound anti-CD3 mAb and anti-CD28 mAb for 48 h. Cells were stained with Abs to CTLA-4, BTLA, and PD-1 together with anti-CD4 mAb or anti-CD8 mAb. Numbers indicate percentages of cell population positive for indicated Ags among CD4 or CD8 T cells. FACS analysis from one representative control of seven HC is shown for each subset. A dotted line indicates a control staining with isotype-matched Ab. *D*, Pooled data from HC (n = 7) and patients (1 and 2). Percentages of CTLA-4$^+$, BTLA$^+$, and PD1$^+$ CD4 T cells among CD4 T cells and that of PD-1$^+$ CD8 T cells among CD8 T cells from HC and ICOS-deficient patients (1 and 2) after CD3/CD28 stimulation are shown. The FACS analysis was conducted three times for the patients, and average percentages were plotted. Error bar indicates SD.

anti-CD28, and the cells were examined at the end of incubation for the expression of TNF/TNFR family proteins (TNFRI (CD120a), TNFRII (CD120b), CD40L, OX40, and 4-1BB) and of CD28 family proteins (CTLA-4, BTLA, and PD1 (CD279)).

The analysis revealed that CD40L expression was induced normally in the patients' CD4 T cells, indicating that the hyper-IgM phenotype observed in patient 2 was not due to defective induction of CD40L.

T cells were fully activated in the patients at the end of CD3/CD28 stimulation, as evidenced by CD69 Ag expression. The levels of OX40, 4-1BB, TNFRI, and TNFRII were normal on the surface of the T cells in the ICOS-deficient patients (Fig. 4, *A* and *B*, and data not shown).

Baseline CD28 expression in CD4 T cells was similar to that of healthy subjects (data not shown). In contrast, the frequency of CTLA-4$^+$ CD4 T cells after CD3/CD28 costimulation was markedly reduced in the patients (Fig. 4*C*). Combined data from seven age-matched controls showed that CTLA-4 was induced in 47.4 ± 4.9% of CD4 T cells. In contrast, induction was observed in 30.1 and 24.6% of CD4 T cells in patients 1 and 2, respectively (Fig. 4, *C* and *D*). Moreover, as seen in the representative plot in Fig. 4*C*, the expression level of CTLA-4 in the CTLA-4$^+$ population was also diminished in the patients.

Induction of BTLA, another inhibitory receptor with similarities to CTLA-4 (5), was then estimated. The average percentage of BTLA$^+$ CD4 T cells was slightly lower in the patients (22.0% for

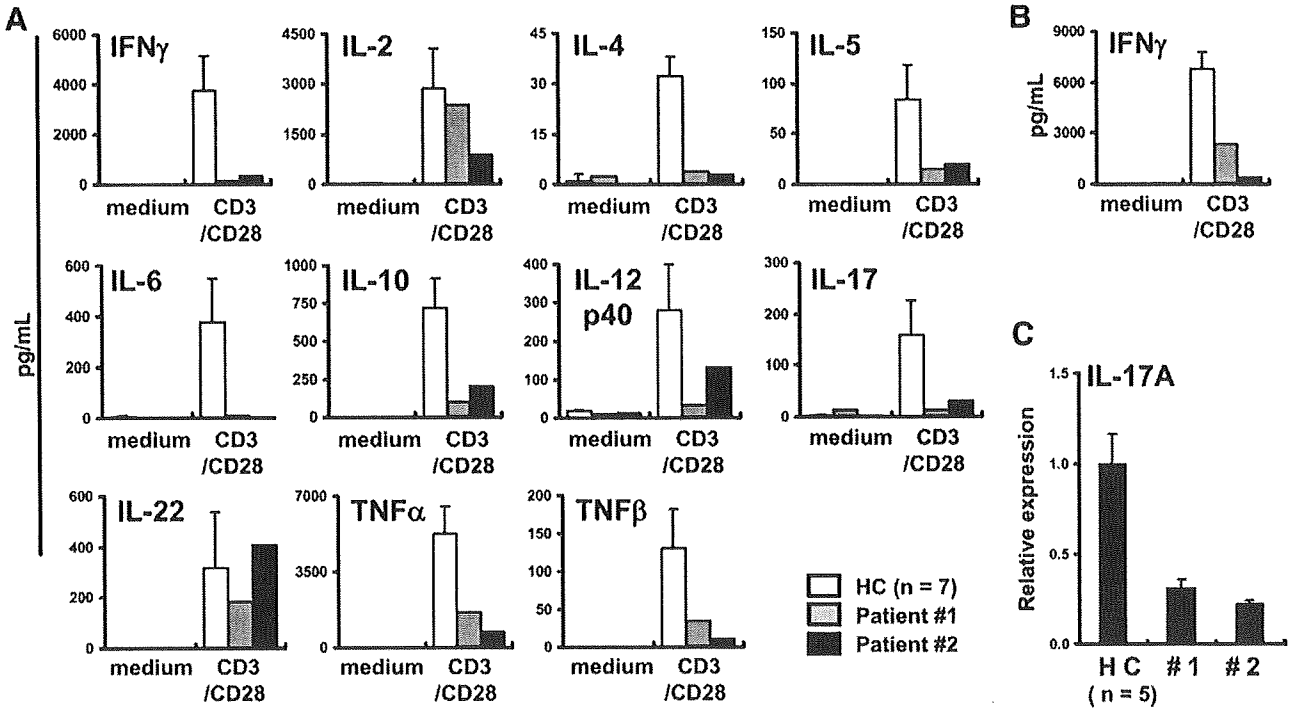

FIGURE 5. Impaired cytokine production in ICOS-deficient patients. *A*, Purified CD4 T cells were stimulated with plate-bound anti-CD3 mAb and anti-CD28 mAb for 24 h or in a medium, and the levels of cytokines in the supernatants were measured by ELISA, FlowCytomix, or both. Error bars for healthy controls (HC, $n = 7$) indicate SD. Experiments were repeated at least twice for the patients, and mean concentrations were plotted. *B*, Purified CD8 T cells were stimulated as in *A*, and the levels of IFN-γ in the supernatants were measured by FlowCytomix. □, HC; ▨, patient 1; ■, patient 2. Error bars for HC ($n = 5$) indicate SD. Experiments were repeated twice for the patients, and mean concentrations were plotted. *C*, IL-17A mRNA expression. The level of IL-17A mRNA was measured in anti-CD3/anti-CD28-stimulated $CD4^+$ T cells by real-time PCR. Relative mRNA level of IL-17A was calculated using GAPDH expression as a reference, and the mean expression level for HC ($n = 5$) was adjusted to 1.0. Error bar indicates SD. IL-17A mRNA expression for the patients was measured three times, and is expressed as mean ± SEM.

patient 1; 21.4% for patient 2) compared with controls (34.0 ± 8.7%, $n = 7$) (Fig. 4, *C* and *D*).

In the patients, the frequency of CD4 T cells bearing PD1, a molecule that plays a critical role in the induction and/or maintenance of T cell tolerance (1), was similar to that in controls (Fig. 4, *C* and *D*). The percentages of $PD1^+$ CD8 T cells, which function as inhibitory T cells (43), were slightly reduced only in patient 2 (29.0%) compared with controls (49.8 ± 9.0%, $n = 7$).

Impaired production of cytokines in ICOS-deficient patients

We next assessed the production of a panel of cytokines by a FlowCytomix bead-based multiplex assay, ELISA, or both, after incubation of CD4 T cells purified to >95% with costimulation of the TCR-CD3 complex via CD28.

In contrast to previous data obtained in other cases of human ICOS deficiency, the production of IFN-γ (Th1 cytokine) and IL-4 and IL-5 (Th2 cytokines) was significantly reduced (Fig. 5*A*) in the patients than in controls (31, 33). Secretion of IL-10 and IL-17 was impaired in the ICOS-deficient patients, in agreement with the previous report (33). To confirm the Th17 defect in the patients, a real-time PCR analysis was used to quantify IL-17A mRNA induction. The results, shown in Fig. 5*C*, demonstrate a significant decrease in relative IL-17A mRNA expression in ICOS-deficient T cells. Furthermore, induction of other cytokines, such as IL-6, IL-12 p40, TNF-α, and TNF-β, in CD4 T cells was impaired to various degrees in the patients (Fig. 5*A*).

Interestingly, the synthesis of the different cytokines was not equally affected in the absence of ICOS: the production of IL-2 was within ±1 SD of normal values, and the IL-22 response was similar to that in controls.

To determine whether the observed defects in effector T cell function can be reproduced by direct activation of intracellular signaling, we examined the capacity of lymphocytes to produce cytokines after PMA/ionomycin stimulation. To that end, intracellular IFN-γ, IL-4, and IL-17 were monitored in PBMCs stimulated with PMA/Ca ionophore by flow cytometry. Fig. 6*A* shows that the CD4 T cells of the patients elicited markedly reduced Th1, Th2, and Th17 cytokine responses.

To corroborate these results, we measured the level of cytokines using a FlowCytomix kit in purified CD4 T cells incubated with PMA and ionomycin for 24 h. A similar trend was noted, as follows: the production of IFN-γ, IL-5, IL-10, TNF-α, and TNF-β was found to be diminished. The capacity of $ICOS^{-/-}$ CD4 T cells to produce IL-2 and IL-6, however, was not markedly impaired (supplemental Fig. 1).[3]

Because $CD45RO^+$ T cells are the major producers of IFN-γ, IL-4, and IL-17 (44) (Fig. 6*A*), we considered the possibility that the impaired cytokine responses were due to the decrease in memory CD4 T cells in the patients. To test this, we stimulated PBMCs with PMA/ionomycin and tested for intracellular IFN-γ, IL-4, or IL-17 in the $CD4^+CD45RO^+$ population. Fig. 6, *A* and *B*, shows that memory T cells of the patients produced less IFN-γ than the controls. In the controls, 30% of $CD45RO^+$ memory T cells produced IFN-γ, whereas in the patients, only ~10% of $CD45RO^+$ memory T cells did so. The synthesis of IL-4 and IL-17 in the memory T cell fraction was marginally decreased in the patients,

[3] The online version of this article contains supplemental material.

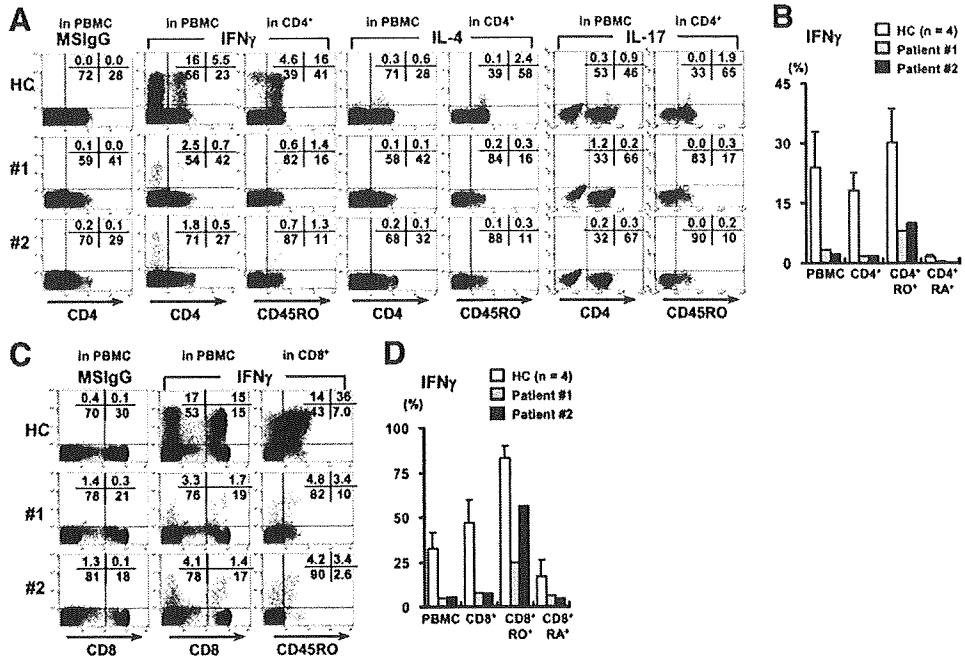

FIGURE 6. Defective cytokine production in T cells stimulated with PMA/ionomycin in ICOS-deficient patients. *A* and *C*, PBMCs were stimulated with PMA and ionomycin for 5 (IL-17) or 8 h (IFN-γ and IL-4). Cells were stained for intracellular IFN-γ, IL-4, and IL-17 together with Abs to CD4 and CD45RO or CD45RA. The same experiment was conducted in CD8 T cells for intracellular detection of IFN-γ. Intracellular staining of each cytokine in CD4 and $CD4^+CD45RO^+$ T cells (*A*) and in CD8 and $CD8^+CD45RO^+$ T cells (*C*) is shown. A representative FACS analysis is illustrated for one of four healthy controls (HC) (for CD4), one of five HC (for CD8), and the patients. *B* and *D*, Pooled data on IFN-γ-producing cells among PBMCs, CD4 T cells, $CD4^+CD45RO^+$ cells, $CD4^+CD45RA^+$ cells, CD8 T cells, and $CD8^+CD45RO^+$ cells, in HC ($n = 4$) and patients 1 and 2. □, HC; ▨, patient 1; ■, patient 2. Error bar for HC indicates SD. The mean percentage obtained from two separate analyses is shown for the patients.

and the decline was not as clear as that observed in IFN-γ production (Fig. 6*A*).

Importantly, the inability to produce IFN-γ does not seem to be restricted to CD4 T cells, because a marked reduction in the IFN-γ response was also evident in the CD4-negative population. To assess effector function of CD8 T cells, we directly measured intracellular IFN-γ in CD8 T cells and a $CD8^+CD45RO^+$ population upon stimulation with PMA/ionomycin. The results displayed in Fig. 6, *C* and *D*, revealed impaired IFN-γ production from CD8 T cells and memory CD8 T cells from the patients. The production of IFN-γ was also significantly reduced in CD8 T cells stimulated through CD3 and CD28 in the patients (Fig. 5*B*).

Mechanism of defective cytokine production in patients: reduced induction of master regulators of Th1, Th2, and Th17 lineage commitment

We next investigated the mechanisms underlying the T cell unresponsiveness in the patients. One potential explanation is that their T cells did not proliferate well or were prone to apoptosis, or both, in the absence of ICOS expression. To examine this possibility, the proportion of cells that underwent PMA/ionophore-induced cell death was assessed by annexin V/7-AAD staining. The results showed that in the patients, this proportion was similar to or rather lower than that in controls. The proliferative capacity of $ICOS^{-/-}$ T cells, as assessed by CFSE staining, showed that their T cells proliferated normally or even more vigorously in response to CD3/CD28 cosignal, with significantly more cells with multiple divisions, relative to controls (supplemental Fig. 2).[3]

Although less likely, the absence of the ICOS-ICOS-L interaction during CD3/CD28 costimulation of CD4 T cells may have contributed to impaired cytokine production in the patients. To test the possible contribution of the ICOS signal in cytokine production, we stimulated purified CD4 T cells from healthy controls ($n = 5$) through CD3/CD28 with or without anti-ICOS-L blocking Ab (45), and measured the level of cytokines in the supernatants. Supplemental Fig. 3, *A–C*,[3] shows that the effect of ICOS blocking is negligible in this cytokine production assay.

Another explanation for the defective production of effector cytokines is that there were fundamental flaws in their development into effector T cell subsets. We therefore investigated the expression of master transcription regulators of Th1, Th2, and Th17 lineage commitments by quantitative real-time PCR.

Purified CD4 T cells were stimulated with PMA/ionomycin for 4 h or anti-CD3/CD28 for 24 h, and the mRNA expression level of T-bet (for the Th1 lineage) (46), GATA3 and MAF (for the Th2 lineage) (47, 48), and RORC/ROR-γt (for the Th17 lineage) (49) was quantified using GAPDH expression as a control, and expressed as relative expression (RE) adjusted for the baseline expression level of healthy controls ($n = 4$), taken as 1.0. We observed reduced PMA/ionophore-driven T-bet induction in $ICOS^{-/-}$ CD4 T cells in the patients, and defective induction was more pronounced in patient 2 (Fig. 7*A*). Compared with controls (RE, 16.2 ± 5.3), CD3/CD28-induced T-bet expression was decreased in patient 1 (RE, 7.2), whereas the reduction was less marked in patient 2 (RE, 12.4) (Fig. 7*B*).

GATA-3 induction was detectable after PMA/ionophore stimulation. In the patients, induction of GATA-3 above the baseline level was virtually absent in CD4 T cells (RE, 1.3 for patient 1, and 1.0 for patient 2) (Fig. 7*A*). The RE values of MAF in CD4 T cells in response to PMA/ionomycin and TCR/CD28 in controls were 3.3 ± 1.4 and 4.4 ± 1.0, respectively. In contrast, stimulation-induced MAF expression was virtually absent in both patients (Fig. 7, *A* and *B*).

We also observed that the expression levels of RORC in ICOS-deficient CD4 T cells stimulated with CD3/CD28 or PMA/ionomycin were diminished more than 2-fold (Fig. 7, *A* and *B*).

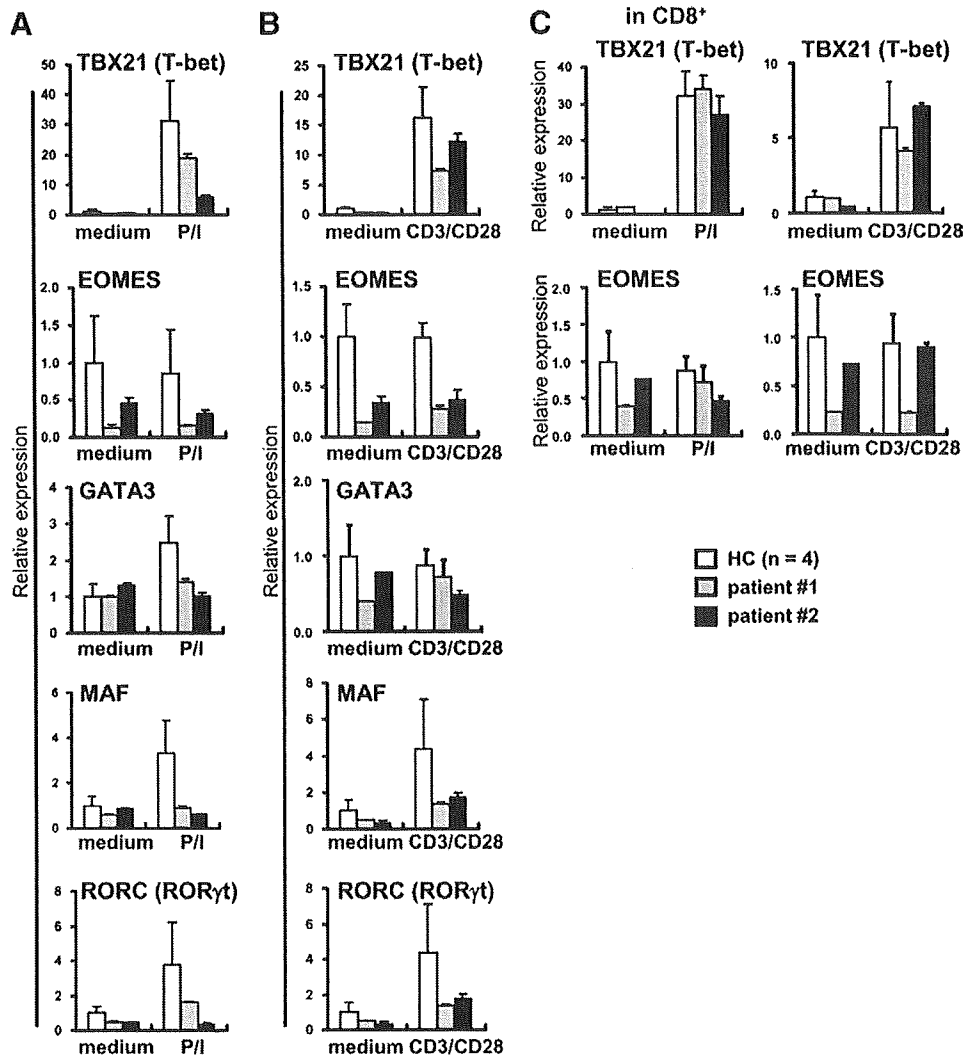

FIGURE 7. Impaired expression of effector-specific transcription factors for T cell differentiation. Purified CD4 T cells were activated by PMA/ionomycin or incubated in the medium for 4 h (*A*), or were incubated in the presence or absence of anti-CD3/anti-CD28 costimulation for 24 h (*B*). Expression levels of TBX21 (T-bet), GATA-3, MAF, RORC (ROR-γt), and EOMES mRNAs were determined in duplicate by real-time quantitative PCR. Similarly, purified CD8 T cells were activated by PMA/ionomycin or by anti-CD3/anti-CD28; and the expression levels of TBX21 and EOMES were assessed in healthy controls (HC). Patients 1 and 2 (*C*). Levels of each mRNA were expressed as relative expression compared with expression of 18S rRNA, and the mean mRNA expression level in cells from HC cultured in the medium was adjusted to 1.0. □, HC; ▨, patient 1; ■, patient 2. Error bars indicate the SD for HC (n = 5). The assay was performed three times for the patients; average and SEM are shown. P/I: PMA/ionomycin.

Despite poor IFN-γ production by CD8 T cells, we did not observe low T-bet induction in purified CD8 T cells when stimulated by PMA/ionomycin or by anti-CD3/anti-CD28 mAb (Fig. 7*C*). We then tested the expression of EOMES, a paralog of T-bet and a transcription factor required for CD8 effector function (50, 51). Although induction was negligible, there was a trend toward lower baseline expression of EOMES (0.23 and 0.69 for patients 1 and 2, respectively).

Expression of the E3 ubiquitin ligases that contribute to T cell anergy

Several lines of evidence indicate that E3 ubiquitin ligases (Grail, Cbl-b, and Itch) play important roles in the induction and maintenance of T cell tolerance (52–55). T cell stimulation without costimulation leads to up-regulation of these ligases (56). High expression of these E3 ubiquitin ligases is related to the absence of the expression of the effector-specific transcription factors (56, 57). There has been little research on the ligases in human systems. Because anti-CD3 stimulation did not induce appreciable up-regulation of the ligases, we examined the mRNA level of these molecules at baseline and after PMA/ionophore stimulation using a sensitive real-time PCR assay.

As shown in Fig. 8, baseline expression of the E3 ubiquitin ligases, with the exception of Grail, was detected in the controls and patients. The mRNA levels of Cbl-b and AIP4/Itch in the steady state were significantly elevated in patient 2 (2.5 and 4.3) compared with controls (1.0 ± 0.4 and 1.0 ± 0.6, n = 4) and patient 1 (1.0 and 1.3).

PMA/ionophore induced up-regulation of Cbl-b and Itch, but not Grail, in normal subjects, whereas the induction of Cbl-b and Itch mRNA above the baseline level was negligible in patient 2 (Fig. 8).

Of particular note was a paradoxical down-regulation of Itch, a regulator of NF-κB activation, upon PMA/ionophore stimulation, which was reproducibly observed only in patient 1.

RANKL induction was augmented in patient 2 with autoimmunity

Patient 1 had an autoimmune manifestation and immunodeficiency, whereas patient 2 had mild psoriasis-like cutaneous lesions and mild skin infections. We therefore attempted to uncover differences in T cell functions between two patients.

To explore the dissimilarities in their immune functions, we assessed mRNA expression levels in negatively selected, >97% pure CD4 T cells by comprehensive mRNA expression analysis using a GeneChip before and after stimulation through CD3/CD28.

The expression of most mRNAs from CD4 T cells poststimulation showed a remarkably high correlation between patients 1 and 2. However, we identified >100 genes that were differently expressed between the patients, and sought to identify the gene(s) that may explain the phenotypic difference from these genes.

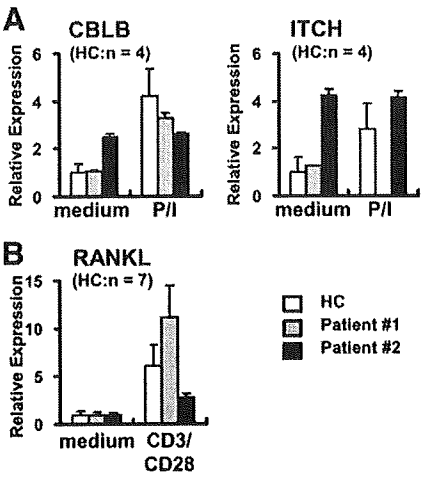

FIGURE 8. *A*, Expression levels of E3 ubiquitin ligases. Cbl-b and Itch mRNA levels were measured by real-time RT-PCR, as indicated in Fig. 5. Purified CD4 T cells from healthy controls (HC; $n = 4$) and patients (1 and 2) were activated with PMA/ionomycin or incubated in the medium only for 4 h. mRNA levels for Cbl-b and Itch were quantified in duplicate with 18S rRNA as a reference, and baseline expression in HC was adjusted to 1.0. Error bars indicate SD for HC and SEM for patients. Expression of Grail (RNF128) was not detectable before or after stimulation in this assay (data not shown). *B*, Level of RANKL mRNA expression. CD4 T cells from HC ($n = 7$) and patients (1 and 2) were stimulated with anti-CD3/anti-CD28 mAb, and RANKL mRNA expression was measured. Expression was quantified with 18S RNA as a reference, and the mean expression level of HC was adjusted to 1.0. □, HC; ▨, patient 1; ■, patient 2. Error bars indicate SD for controls and SEM for patients. P/I: PMA/ionomycin.

Among them, TNFSF11 (RANKL) showed >2-fold higher expression in patient 1 after stimulation. In addition, RANKL expression was >50% higher in patient 1 than in the controls.

Because RANKL was identified as a candidate key molecule involved in the pathogenesis of RA (58, 59), we quantified RANKL mRNA in CD3/CD28-stimulated CD4 T cells by real-time PCR. The result shown in Fig. 8*B* demonstrates that compared with healthy controls, RANKL induction was higher in patient 1, but lower in patient 2.

Discussion

In this study, we describe broad defects in T cell function in two siblings with a novel deficiency of human ICOS. Most of the abnormalities presented in this study have not been reported in humans, and some have not been reported in the murine model of ICOS deficiency.

The marked decline in two T cell subpopulations, memory CD4 T cells and CTLA-4$^+$CD45RO$^+$ Tregs, can be explained, at least in part, by a recent observation that the ICOS-ICOS-L interaction plays an important role in the expansion and survival of these effector T cells (23, 60).

With regard to CD4 memory T cells, we observed significant reductions in the numbers of both TCMs and TEMs in the steady state, which were not observed in the previously reported cases of human ICOS deficiency (31–33). A reduction in the number of TEMs, but not of TCMs, was demonstrated in ICOS knockout mice by Burmeister et al. (23). TEMs were decreased up to 4-fold in the steady state; the decrease was more pronounced in older mice. TEMs and TCMs display significant and intermediate ICOS expression, respectively (23). Through detailed research on expansion, differentiation, and survival of effector T cells in the absence of ICOS, they suggested that ICOS controls the pool size of effector T cells. These data suggest that both memory subsets may require ICOS for proliferation and survival in humans. Therefore, a decline in total memory cells may be observed in ICOS-deficient mice over a longer observation period and/or after recurrent infections. Alternatively, it is equally plausible that the ICOS-ICOS-L interaction plays a pivotal role in commitment to memory T cells.

CTLA-4$^+$CD45RO$^+$ICOS$^+$CD4$^+$CD25$^+$ Tregs, commonly observed in adults, were virtually absent in our ICOS-deficient patients. The reduction was seemingly counterbalanced by an increased number of CTLA-4$^-$CD45RO$^-$ Tregs. Although the contribution of ICOS to the expansion and maintenance of Tregs as a whole has been previously reported (23, 41), our observation addresses the role of ICOS in the maintenance of an IL-10-producing memory subset of Tregs, but not TGF-β-producing CTLA-4$^-$CD45RO$^-$ICOS$^-$ naive Tregs. Supporting this is the observation that in mice, ICOS$^+$ Tregs display a strict propensity to undergo rapid apoptosis in culture unless signaled by ICOS-L (23).

The decrease in the number of CTLA-4$^+$ Tregs may be alternatively explained by defective induction of a gene that regulates Treg development. A recent study in mice has demonstrated that ROR-γt controls the development of IL-10-producing Tregs that coexpress ICOS in addition to CCL20 (61). This finding may suggest that the decrease in CTLA-4$^+$CD45RO$^+$FoxP3$^+$ Tregs is a consequence of reduced induction of ROR-γt/RORC, as observed in the present study.

Another notable T cell defect in our patients was the impaired capacity of their T cells to mount Th1, Th2, and Th17 responses. Reduced cytokine production was observed not only when the patients' CD4 T cells were activated by costimulatory signals, but also when they were stimulated by PMA/ionomycin.

Although the ICOS-ICOS-L interaction was important in vivo in the generation and/or maintenance of effector memory and central memory cells, the absence of an ICOS signal through ICOS-L did not seem to contribute to the T cell effector defects observed in our ex vivo experiments. First, ICOS-L expression was not induced in purified T cells upon CD3/CD28 costimulation (supplemental Fig. 3*A*).[3] In addition, blocking potential ICOS-ICOS-L interaction in the controls did not result in decreased cytokine production or in decreased up-regulation of MAF and RORC (supplemental Fig. 3, *B* and *C*).[3]

Additional experiments indicated that there was an abnormality at the level of transcriptional regulation of Th1, Th2, and Th17 polarization, and decreased induction of the master regulators T-bet, GATA-3, MAF, and RORC in the patients. Previous research on mice has shown that ICOS regulates MAF expression and GATA-3 induction (62), and our present study points to an additional role of ICOS in the complete induction of T-bet and RORC.

One major factor contributing to the poor effector T cell responses in the patients could be the decrease in total memory CD4 T cells. This is particularly likely in the case of IL-4 and IL-17 production, because the memory T cells had only mild defect in producing IL-4 and IL-17. Although the CD4$^+$CD45RO$^+$ T cells in the patients displayed a significantly reduced ability to produce IFN-γ, the decreased response may be explained by pronounced reduction in TEMs in the patients. To determine whether the memory T cell compartment in our patients is functionally defective or intact on a per cell basis, we would need further analysis of various parameters of the T cell effector functions in naive T cells, TCMs, and TEMs.

Nurieva et al. (56) demonstrated that murine ICOS$^{-/-}$ CD4 T cells showed defective induction of T-bet, GATA-3, and EOMES in the absence of CD28 costimulation because of up-regulation of E3 ubiquitin ligases: Grail, Cbl-b, and Itch. It is uncertain whether the augmented baseline expression of E3 ubiquitin ligases is relevant to the observed effector T cell dysfunction, because this was

confirmed only in patient 2. It is rather unlikely that the different expression of the E3 ubiquitin ligases contributed to the T cell defects in the patients because augmented induction of these ligases was not detected in the patients.

In contrast to the global impairment in cytokine synthesis, IL-2 production was only marginally affected. Supporting this observation, induction of transcription factors for IL-2 (c-Jun/c-Fos) was normal in the patients (data not shown). Similarly, induction of IL-21 and TGF-β was also unaffected in the CD4 T cells of the patients, although their induction was modest under costimulatory conditions (data not shown). It should be noted that production of IL-22, a Th17 cytokine fundamental for the development of psoriasis, showed normal induction, and that both the patients had psoriatic cutaneous lesions (63). Although whether IL-17A and IL-22 are produced by the same Th17 subset is still unclear (64, 65), our data suggest an IL-22-producing CD4 T cell subset is not functionally impaired in the patients.

Previous studies in mice have shown that ICOS is necessary for optimal CD8 T cell responses (34). ICOS can directly stimulate CD8 T cells (35); and ICOS-Ig-treated mice displayed diminished IFN-γ production by CD8 T cells. Our study has demonstrated that CD8 memory cells are reduced in ICOS deficiency, and that CD8 T cells in the absence of ICOS can mount a very low IFN-γ response, for the first time in humans. ICOS is induced on terminally differentiated $CD28^{-}CD8$ effector T cells (11), and thus, may play a role in maintaining the CD8 subset. Therefore, a decrease in the number of IFN-γ-producing CD8 T cells could be ascribed to the reduction in $CD45RO^{+}$ memory CD8 T cells or in $CD28^{-}CD8$ T cells (data not shown) in our ICOS-deficient patients. IFN-γ production is regulated by T-bet and EOMES cooperatively or redundantly in CD8 T cells (50, 51). T-bet induction was normal when stimulated with PMA/ionomycin or anti-CD3/anti-CD28, whereas a baseline expression of EOMES was decreased in CD8 T cells in the patients. Although this may explain the impaired production in part, further research on the CD8 T cells stimulated with various common γ-chain cytokines would be necessary to assess whether the transcriptional regulation of CD8 effector functions is impaired in the absence of ICOS.

In addition to the reduced numbers of effector T cells, which either potentiate or inhibit T cell responses, the present study demonstrates for the first time an aberrant induction of negative costimulatory molecules on activated T cells in ICOS-deficient patients. CTLA-4 and BTLA are induced upon activation and transmit an inhibitory signal to T cells to regulate the balance between T cell activation, tolerance, and immunopathology (3–5). Costimulatory and coinhibitory molecules are normally induced in the absence of ICOS in mice and humans (23, 31). In our patients, however, induction of CTLA-4 and BTLA following CD3/CD28 signaling was impaired. Although the molecular basis of the defective expression is still not known, this may be ascribed to the decreased memory T cell subset in the patients. At all events, our findings imply that an inhibitory signal to suppress activated T cells could not be appropriately induced in the patients.

Collectively, these data highlight the positive contribution of ICOS to the maintenance of, or commitment to, effector T cells and a subset of Tregs, and the induction of negative costimulatory receptors on activated T cells. The immunodeficiency in our ICOS-deficient patients, although mild, can be understood by the defects in their effector T cell functions as well as in T cell-dependent B cell help, but a reasonable explanation is still required for the development of autoimmunity, RA, IBD, IP, and psoriasis in ICOS-deficient patients.

Most studies have depicted ICOS as a positive costimulator in the immune reaction. For example, research in ICOS-deficient mice suggests that ICOS is critically involved in autoimmune development and allogeneic reactions (21, 25–29). There are, however, some results indicating that abrogation of the ICOS-ICOS-L interaction aggravates the disease process. For example, in some initial studies on ICOS-null mice, experimental autoimmune encephalomyelitis was unexpectedly exacerbated and allergen-dependent airway sensitivity was augmented (14, 66, 67). What is the role of ICOS in autoimmune development?

Burmeister et al. (23) reported that ICOS supports the expansion and survival of Th1 or Th2 responder cells, Th17 cells, and $FoxP3^{+}$ regulatory effector cells. They hypothesized that the absence of ICOS function in a particular mouse model would result in a phenotype reflecting a deficiency of the dominant effector T cell type. Thus, blockade of the ICOS-ICOS-L interaction could mainly affect Treg subsets and lead to the development of autoimmune disorders.

Our observations in human ICOS deficiency may fit the concept of ICOS as an agonist molecule. In our ICOS-deficient patients, defects in T cell function leading to termination of the activated T cell response may have been dominant.

Another question remains, as we observed a wide range of autoimmune diseases in patient 1, but not in patient 2. Although phenotypic variation in siblings with the same mutation is not uncommon in human genetic disorders, there might have been some contributing factor(s).

First, our analysis showed paradoxical down-regulation of Itch expression after PMA/ionophore stimulation in patient 1. Because Itch induction is important in the control of NF-κB activation (55), an activation signal in the absence of CD28 costimulation may have led to continuous inflammation in patient 1.

Second, although the T cell immune functions and stimulation-induced mRNA expression pattern of CD4 T cells were strikingly similar between the siblings, we found that the T cells of patient 1 showed exaggerated induction of RANKL expression and poorer production of IFN-γ. Previous studies demonstrated that T cells, which contribute to the development of RA and IBD, were characterized by poor IFN-γ production, production of inflammatory cytokines including IL-17A and TNF, and RANKL expression (59). Although IL-17A induction was not increased, the augmented RANKL expression and poor IFN-γ production in T cells may have contributed to the autoimmune disease progression. Characterization of RANKL-expressing IL-17A-negative T cells requires further investigation.

Third, we surmised that a major infectious episode may have upset the subtle balance between effector T cells and Tregs in our patients. In fact, patient 1 developed a series of autoimmune disorders after a severe bacterial infection.

Finally, the reason for the apparent discrepancy in T cell functions between the ICOS-deficient patients presented in this study and the ICOS deficiency described in previous reports (31–33) is elusive. One possibility that explains the difference in cytokine production in our patients and ICOS deficiency in previous reports could be different stimulation condition (dose of mAb and incubation period). However, it is unlikely because effective cytokine synthesis from the T cells was not observed in our patients even with an increased dose of anti-CD28 mAb and with longer time periods (supplemental Fig. 4).[3] This indicates the presence of other intrinsic factor(s).

Another possibility is the difference in the mutation site of the ICOS gene. Our patients harbored a homozygous single-base deletion at codon 285 located in the extracellular domain, whereas other ICOS deficiencies have homozygous deletion in exons 2 and 3 of the ICOS gene (33). In addition to defective ICOS expression,

this mutation may result in the expression of a 120-aa ICOS protein that affects immune function, for example, by binding to ICOS-L on B cells, monocytes, or a subset of T cells. Despite extensive investigation, however, we have been unable to demonstrate the expression of a truncated ICOS protein in our patients' lymphocytes.

In summary, the present study on T cell functions in two novel ICOS-deficient patients has shown that the interaction between ICOS and ICOS-L is critical for the development and maintenance of multiple types of effector cells and Tregs, and that the defects are at least in part due to diminished memory T cells and/or impaired induction of master regulators. Collectively, the results of our study highlight a major role of ICOS as a coordinator of T cell immune responses and T cell maintenance.

Acknowledgments

We thank Nakaba Ochiai and Shizuko Minegishi for technical assistance, and Drs. Erdyni Tsitsikov and Jun-ichi Yata for critical reading of the manuscript.

Disclosures

The authors have no financial conflict of interest.

References

1. Greenwald, R. J., G. J. Freeman, and A. H. Sharpe. 2005. The B7 family revisited. *Annu. Rev. Immunol.* 23: 515–548.
2. Rudd, C. E., and H. Schneider. 2003. Unifying concepts in CD28, ICOS and CTLA4 co-receptor signalling. *Nat. Rev. Immunol.* 3: 544–556.
3. Chen, L. 2004. Co-inhibitory molecules of the B7-CD28 family in the control of T-cell immunity. *Nat. Rev. Immunol.* 4: 336–347.
4. Leibson, P. J. 2004. The regulation of lymphocyte activation by inhibitory receptors. *Curr. Opin. Immunol.* 16: 328–336.
5. Watanabe, N., M. Gavrieli, J. R. Sedy, J. Yang, F. Fallarino, S. K. Loftin, M. A. Hurchla, N. Zimmerman, J. Sim, X. Zang, et al. 2003. BTLA is a lymphocyte inhibitory receptor with similarities to CTLA-4 and PD-1. *Nat. Immunol.* 4: 670–679.
6. Coyle, A. J., and J. C. Gutierrez-Ramos. 2001. The expanding B7 superfamily: increasing complexity in costimulatory signals regulating T cell function. *Nat. Immunol.* 2: 203–209.
7. Keir, M. E., and A. H. Sharpe. 2005. The B7/CD28 costimulatory family in autoimmunity. *Immunol. Rev.* 204: 128–143.
8. Salzer, U., and B. Grimbacher. 2006. Common variable immunodeficiency: the power of co-stimulation. *Semin. Immunol.* 18: 337–346.
9. Yoshinaga, S. K., J. S. Whoriskey, S. D. Khare, U. Sarmiento, J. Guo, T. Horan, G. Shih, M. Zhang, M. A. Coccia, T. Kohno, et al. 1999. T-cell co-stimulation through B7RP-1 and ICOS. *Nature* 402: 827–832.
10. Coyle, A. J., S. Lehar, C. Lloyd, J. Tian, T. Delaney, S. Manning, T. Nguyen, T. Burwell, H. Schneider, J. A. Gonzalo, et al. 2000. The CD28-related molecule ICOS is required for effective T cell-dependent immune responses. *Immunity* 13: 95–105.
11. Hutloff, A., A. M. Dittrich, K. C. Beier, B. Eljaschewitsch, R. Kraft, I. Anagnostopoulos, and R. A. Kroczek. 1999. ICOS is an inducible T-cell co-stimulator structurally and functionally related to CD28. *Nature* 397: 263–266.
12. Kroczek, R. A., H. W. Mages, and A. Hutloff. 2004. Emerging paradigms of T-cell co-stimulation. *Curr. Opin. Immunol.* 16: 321–327.
13. McAdam, A. J., T. T. Chang, A. E. Lumelsky, E. A. Greenfield, V. A. Boussiotis, J. S. Duke-Cohan, T. Chernova, N. Malenkovich, C. Jabs, V. K. Kuchroo, et al. 2000. Mouse inducible costimulatory molecule (ICOS) expression is enhanced by CD28 costimulation and regulates differentiation of $CD4^+$ T cells. *J. Immunol.* 165: 5035–5040.
14. Dong, C., A. E. Juedes, U. A. Temann, S. Shresta, J. P. Allison, N. H. Ruddle, and R. A. Flavell. 2001. ICOS co-stimulatory receptor is essential for T-cell activation and function. *Nature* 409: 97–101.
15. McAdam, A. J., R. J. Greenwald, M. A. Levin, T. Chernova, N. Malenkovich, V. Ling, G. J. Freeman, and A. H. Sharpe. 2001. ICOS is critical for CD40-mediated antibody class switching. *Nature* 409: 102–105.
16. Tafuri, A., A. Shahinian, F. Bladt, S. K. Yoshinaga, M. Jordana, A. Wakeham, L. M. Boucher, D. Bouchard, V. S. Chan, G. Duncan, et al. 2001. ICOS is essential for effective T-helper-cell responses. *Nature* 409: 105–109.
17. Watanabe, M., S. Watanabe, Y. Hara, Y. Harada, M. Kubo, K. Tanabe, H. Toma, and R. Abe. 2005. ICOS-mediated costimulation on Th2 differentiation is achieved by the enhancement of IL-4 receptor-mediated signaling. *J. Immunol.* 174: 1989–1996.
18. Sperling, A. I., and J. A. Bluestone. 2001. ICOS costimulation: it's not just for TH2 cells anymore. *Nat. Immunol.* 2: 573–574.
19. Ozkaynak, E., W. Gao, N. Shemmeri, C. Wang, J. C. Gutierrez-Ramos, J. Amaral, S. Qin, J. B. Rottman, A. J. Coyle, and W. W. Hancock. 2001. Importance of ICOS-B7RP-1 costimulation in acute and chronic allograft rejection. *Nat. Immunol.* 2: 591–596.
20. Gonzalo, J. A., J. Tian, T. Delaney, J. Corcoran, J. B. Rottman, J. Lora, A. Al-garawi, R. Kroczek, J. C. Gutierrez-Ramos, and A. J. Coyle. 2001. ICOS is critical for T helper cell-mediated lung mucosal inflammatory responses. *Nat. Immunol.* 2: 597–604.
21. Rottman, J. B., T. Smith, J. R. Tonra, K. Ganley, T. Bloom, R. Silva, B. Pierce, J. C. Gutierrez-Ramos, E. Ozkaynak, and A. J. Coyle. 2001. The costimulatory molecule ICOS plays an important role in the immunopathogenesis of EAE. *Nat. Immunol.* 2: 605–611.
22. Park, H., Z. Li, X. O. Yang, S. H. Chang, R. Nurieva, Y. H. Wang, Y. Wang, L. Hood, Z. Zhu, Q. Tian, and C. Dong. 2005. A distinct lineage of CD4 T cells regulates tissue inflammation by producing interleukin 17. *Nat. Immunol.* 6: 1133–1141.
23. Burmeister, Y., T. Lischke, A. C. Dahler, H. W. Mages, K. P. Lam, A. J. Coyle, R. A. Kroczek, and A. Hutloff. 2008. ICOS controls the pool size of effector-memory and regulatory T cells. *J. Immunol.* 180: 774–782.
24. Akbari, O., P. Stock, E. H. Meyer, G. J. Freeman, A. H. Sharpe, D. T. Umetsu, and R. H. DeKruyff. 2008. ICOS/ICOSL interaction is required for $CD4^+$ invariant NKT cell function and homeostatic survival. *J. Immunol.* 180: 5448–5456.
25. Iwai, H., Y. Kozono, S. Hirose, H. Akiba, H. Yagita, K. Okumura, H. Kohsaka, N. Miyasaka, and M. Azuma. 2002. Amelioration of collagen-induced arthritis by blockade of inducible costimulator-B7 homologous protein costimulation. *J. Immunol.* 169: 4332–4339.
26. De Jong, Y. P., S. T. Rietdijk, W. A. Faubion, A. C. Abadia-Molina, K. Clarke, E. Mizoguchi, J. Tian, T. Delaney, S. Manning, J. C. Gutierrez-Ramos, et al. 2004. Blocking inducible co-stimulator in the absence of CD28 impairs Th1 and $CD25^+$ regulatory T cells in murine colitis. *Int. Immunol.* 16: 205–213.
27. Scott, B. G., H. Yang, E. Tuzun, C. Dong, R. A. Flavell, and P. Christadoss. 2004. ICOS is essential for the development of experimental autoimmune myasthenia gravis. *J. Neuroimmunol.* 153: 16–25.
28. Hawiger, D., E. Tran, W. Du, C. J. Booth, L. Wen, C. Dong, and R. A. Flavell. 2008. ICOS mediates the development of insulin-dependent diabetes mellitus in nonobese diabetic mice. *J. Immunol.* 180: 3140–3147.
29. Katsumata, Y., M. Harigai, T. Sugiura, M. Kawamoto, Y. Kawaguchi, Y. Matsumoto, K. Kohyama, M. Soejima, N. Kamatani, and M. Hara. 2007. Attenuation of experimental autoimmune myositis by blocking ICOS-ICOS ligand interaction. *J. Immunol.* 179: 3772–3779.
30. Yu, X. Z., Y. Liang, R. I. Nurieva, F. Guo, C. Anasetti, and C. Dong. 2006. Opposing effects of ICOS on graft-versus-host disease mediated by CD4 and CD8 T cells. *J. Immunol.* 176: 7394–7401.
31. Grimbacher, B., A. Hutloff, M. Schlesier, E. Glocker, K. Warnatz, R. Drager, H. Eibel, B. Fischer, A. A. Schaffer, H. W. Mages, et al. 2003. Homozygous loss of ICOS is associated with adult-onset common variable immunodeficiency. *Nat. Immunol.* 4: 261–268.
32. Salzer, U., A. Maul-Pavicic, C. Cunningham-Rundles, S. Urschel, B. H. Belohradsky, J. Litzman, A. Holm, J. L. Franco, A. Plebani, L. Hammarstrom, et al. 2004. ICOS deficiency in patients with common variable immunodeficiency. *Clin. Immunol.* 113: 234–240.
33. Warnatz, K., L. Bossaller, U. Salzer, A. Skrabl-Baumgartner, W. Schwinger, M. van der Burg, J. J. van Dongen, M. Orlowska-Volk, R. Knoth, A. Durandy, et al. 2006. Human ICOS deficiency abrogates the germinal center reaction and provides a monogenic model for common variable immunodeficiency. *Blood* 107: 3045–3052.
34. Mittrucker, H. W., M. Kursar, A. Kohler, D. Yanagihara, S. K. Yoshinaga, and S. H. Kaufmann. 2002. Inducible costimulator protein controls the protective T cell response against *Listeria monocytogenes*. *J. Immunol.* 169: 5813–5817.
35. Vidric, M., W. K. Suh, U. Dianzani, T. W. Mak, and T. H. Watts. 2005. Cooperation between 4-1BB and ICOS in the immune response to influenza virus revealed by studies of CD28/ICOS-deficient mice. *J. Immunol.* 175: 7288–7296.
36. Morio, T., S. H. Hanissian, L. B. Bacharier, H. Teraoka, S. Nonoyama, M. Seki, J. Kondo, H. Nakano, S. K. Lee, R. S. Geha, and J. Yata. 1999. Ku in the cytoplasm associates with CD40 in human B cells and translocates into the nucleus following incubation with IL-4 and anti-CD40 mAb. *Immunity* 11: 339–348.
37. Watanabe, S., K. Terashima, S. Ohta, S. Horibata, M. Yajima, Y. Shiozawa, M. Z. Dewan, Z. Yu, M. Ito, T. Morio, et al. 2007. Hematopoietic stem cell-engrafted NOD/SCID/IL2Rγ null mice develop human lymphoid systems and induce long-lasting HIV-1 infection with specific humoral immune responses. *Blood* 109: 212–218.
38. Kato, A., T. Homma, J. Batchelor, N. Hashimoto, S. Imai, H. Wakiguchi, H. Saito, and K. Matsumoto. 2003. Interferon-α/β receptor-mediated selective induction of a gene cluster by CpG oligodeoxynucleotide 2006. *BMC Immunol.* 4: 8.
39. Bossaller, L., J. Burger, R. Draeger, B. Grimbacher, R. Knoth, A. Plebani, A. Durandy, U. Baumann, M. Schlesier, A. A. Welcher, et al. 2006. ICOS deficiency is associated with a severe reduction of $CXCR5^+CD4$ germinal center Th cells. *J. Immunol.* 177: 4927–4932.
40. Sallusto, F., D. Lenig, R. Forster, M. Lipp, and A. Lanzavecchia. 1999. Two subsets of memory T lymphocytes with distinct homing potentials and effector functions. *Nature* 401: 708–712.
41. Lohning, M., A. Hutloff, T. Kallinich, H. W. Mages, K. Bonhagen, A. Radbruch, E. Hamelmann, and R. A. Kroczek. 2003. Expression of ICOS in vivo defines $CD4^+$ effector T cells with high inflammatory potential and a strong bias for secretion of interleukin 10. *J. Exp. Med.* 197: 181–193.
42. Ito, T., S. Hanabuchi, Y. H. Wang, W. R. Park, K. Arima, L. Bover, F. X. Qin, M. Gilliet, and Y. J. Liu. 2008. Two functional subsets of $FOXP3^+$ regulatory T cells in human thymus and periphery. *Immunity* 28: 870–880.

43. Izawa, A., K. Yamaura, M. J. Albin, M. Jurewicz, K. Tanaka, M. R. Clarkson, T. Ueno, A. Habicht, G. J. Freeman, H. Yagita, et al. 2007. A novel alloantigen-specific $CD8^+PD1^+$ regulatory T cell induced by ICOS-B7h blockade in vivo. *J. Immunol.* 179: 786–796.
44. Krawczyk, C. M., H. Shen, and E. J. Pearce. 2007. Functional plasticity in memory T helper cell responses. *J. Immunol.* 178: 4080–4088.
45. Youngnak-Piboonratanakit, P., F. Tsushima, N. Otsuki, H. Igarashi, K. Omura, and M. Azuma. 2006. Expression and regulation of human CD275 on endothelial cells in healthy and inflamed mucosal tissues. *Scand. J. Immunol.* 63: 191–198.
46. Szabo, S. J., S. T. Kim, G. L. Costa, X. Zhang, C. G. Fathman, and L. H. Glimcher. 2000. A novel transcription factor, T-bet, directs Th1 lineage commitment. *Cell* 100: 655–669.
47. Zheng, W., and R. A. Flavell. 1997. The transcription factor GATA-3 is necessary and sufficient for Th2 cytokine gene expression in CD4 T cells. *Cell* 89: 587–596.
48. Kim, J. I., I. C. Ho, M. J. Grusby, and L. H. Glimcher. 1999. The transcription factor c-Maf controls the production of interleukin-4 but not other Th2 cytokines. *Immunity* 10: 745–751.
49. Ivanov, I. I., B. S. McKenzie, L. Zhou, C. E. Tadokoro, A. Lepelley, J. J. Lafaille, D. J. Cua, and D. R. Littman. 2006. The orphan nuclear receptor RORγt directs the differentiation program of proinflammatory IL-17^+ T helper cells. *Cell* 126: 1121–1133.
50. Pearce, E. L., A. C. Mullen, G. A. Martins, C. M. Krawczyk, A. S. Hutchins, V. P. Zediak, M. Banica, C. B. DiCioccio, D. A. Gross, C. A. Mao, et al. 2003. Control of effector $CD8^+$ T cell function by the transcription factor Eomesodermin. *Science* 302: 1041–1043.
51. Boyman, O., J. F. Purton, C. D. Surh, and J. Sprent. 2007. Cytokines and T-cell homeostasis. *Curr. Opin. Immunol.* 19: 320–326.
52. Anandasabapathy, N., G. S. Ford, D. Bloom, C. Holness, V. Paragas, C. Seroogy, H. Skrenta, M. Hollenhorst, C. G. Fathman, and L. Soares. 2003. GRAIL: an E3 ubiquitin ligase that inhibits cytokine gene transcription is expressed in anergic $CD4^+$ T cells. *Immunity* 18: 535–547.
53. Bachmaier, K., C. Krawczyk, I. Kozieradzki, Y. Y. Kong, T. Sasaki, A. Oliveira-dos-Santos, S. Mariathasan, D. Bouchard, A. Wakeham, A. Itie, et al. 2000. Negative regulation of lymphocyte activation and autoimmunity by the molecular adaptor Cbl-b. *Nature* 403: 211–216.
54. Heissmeyer, V., F. Macian, S. H. Im, R. Varma, S. Feske, K. Venuprasad, H. Gu, Y. C. Liu, M. L. Dustin, and A. Rao. 2004. Calcineurin imposes T cell unresponsiveness through targeted proteolysis of signaling proteins. *Nat. Immunol.* 5: 255–265.
55. Shembade, N., N. S. Harhaj, K. Parvatiyar, N. G. Copeland, N. A. Jenkins, L. E. Matesic, and E. W. Harhaj. 2008. The E3 ligase Itch negatively regulates inflammatory signaling pathways by controlling the function of the ubiquitin-editing enzyme A20. *Nat. Immunol.* 9: 254–262.
56. Nurieva, R., S. Thomas, T. Nguyen, N. Martin-Orozco, Y. Wang, M. K. Kaja, X. Z. Yu, and C. Dong. 2006. T-cell tolerance or function is determined by combinatorial costimulatory signals. *EMBO J.* 25: 2623–2633.
57. Mueller, D. L. 2004. E3 ubiquitin ligases as T cell anergy factors. *Nat. Immunol.* 5: 883–890.
58. Takayanagi, H., K. Ogasawara, S. Hida, T. Chiba, S. Murata, K. Sato, A. Takaoka, T. Yokochi, H. Oda, K. Tanaka, et al. 2000. T-cell-mediated regulation of osteoclastogenesis by signalling cross-talk between RANKL and IFN-γ. *Nature* 408: 600–605.
59. Sato, K., A. Suematsu, K. Okamoto, A. Yamaguchi, Y. Morishita, Y. Kadono, S. Tanaka, T. Kodama, S. Akira, Y. Iwakura, et al. 2006. Th17 functions as an osteoclastogenic helper T cell subset that links T cell activation and bone destruction. *J. Exp. Med.* 203: 2673–2682.
60. Mahajan, S., A. Cervera, M. MacLeod, S. Fillatreau, G. Perona-Wright, S. Meek, A. Smith, A. MacDonald, and D. Gray. 2007. The role of ICOS in the development of CD4 T cell help and the reactivation of memory T cells. *Eur. J. Immunol.* 37: 1796–1808.
61. Lochner, M., L. Peduto, M. Cherrier, S. Sawa, F. Langa, R. Varona, D. Riethmacher, M. Si-Tahar, J. P. Di Santo, and G. Eberl. 2008. In vivo equilibrium of proinflammatory IL-17^+ and regulatory IL-10^+ $Foxp3^+$ RORγ t^+ T cells. *J. Exp. Med.* 205: 1381–1393.
62. Nurieva, R. I., J. Duong, H. Kishikawa, U. Dianzani, J. M. Rojo, I. Ho, R. A. Flavell, and C. Dong. 2003. Transcriptional regulation of Th2 differentiation by inducible costimulator. *Immunity* 18: 801–811.
63. Zheng, Y., D. M. Danilenko, P. Valdez, I. Kasman, J. Eastham-Anderson, J. Wu, and W. Ouyang. 2007. Interleukin-22, a T_H17 cytokine, mediates IL-23-induced dermal inflammation and acanthosis. *Nature* 445: 648–651.
64. Chung, Y., X. Yang, S. H. Chang, L. Ma, Q. Tian, and C. Dong. 2006. Expression and regulation of IL-22 in the IL-17-producing $CD4^+$ T lymphocytes. *Cell. Res.* 16: 902–907.
65. Scriba, T. J., B. Kalsdorf, D. A. Abrahams, F. Isaacs, J. Hofmeister, G. Black, H. Y. Hassan, R. J. Wilkinson, G. Walzl, S. J. Gelderbloem, et al. 2008. Distinct, specific IL-17- and IL-22-producing $CD4^+$ T cell subsets contribute to the human anti-mycobacterial immune response. *J. Immunol.* 180: 1962–1970.
66. Akbari, O., G. J. Freeman, E. H. Meyer, E. A. Greenfield, T. T. Chang, A. H. Sharpe, G. Berry, R. H. DeKruyff, and D. T. Umetsu. 2002. Antigen-specific regulatory T cells develop via the ICOS-ICOS-ligand pathway and inhibit allergen-induced airway hyperreactivity. *Nat. Med.* 8: 1024–1032.
67. Miyamoto, K., C. I. Kingsley, X. Zhang, C. Jabs, L. Izikson, R. A. Sobel, H. L. Weiner, V. K. Kuchroo, and A. H. Sharpe. 2005. The ICOS molecule plays a crucial role in the development of mucosal tolerance. *J. Immunol.* 175: 7341–7347.

myelogenous leukemia, but are prevalent in chronic myelomonocytic leukemia. *Blood* 1990; **76**: 1214–1219.
4 Loh ML, Martinelli S, Cordeddu V, Reynolds MG, Vattikuti S, Lee CM *et al.* Acquired PTPN11 mutations occur rarely in adult patients with myelodysplastic syndromes and chronic myelomonocytic leukemia. *Leuk Res* 2005; **29**: 459–462.
5 Quesnel B, Preudhomme C, Vanrumbeke M, Vachee A, Lai JL, Fenaux P. Absence of rearrangement of the neurofibromatosis 1 (NF1) gene in myelodysplastic syndromes and acute myeloid leukemia. *Leukemia* 1994; **8**: 878–880.
6 Golub TR, Barker GF, Lovett M, Gilliland DG. Fusion of PDGF receptor beta to a novel ets-like gene, tel, in chronic myelomonocytic leukemia with t(5;12) chromosomal translocation. *Cell* 1994; **77**: 307–316.
7 Lee BH, Tothova Z, Levine RL, Anderson K, Buza-Vidas N, Cullen DE *et al.* FLT3 mutations confer enhanced proliferation and survival properties to multipotent progenitors in a murine model of chronic myelomonocytic leukemia. *Cancer Cell* 2007; **12**: 367–380.
8 Levine RL, Loriaux M, Huntly BJ, Loh ML, Beran M, Stoffregen E *et al.* The JAK2V617F activating mutation occurs in chronic myelomonocytic leukemia and acute myeloid leukemia, but not in acute lymphoblastic leukemia or chronic lymphocytic leukemia. *Blood* 2005; **106**: 3377–3379.
9 Lorenzo F, Nishii K, Monma F, Kuwagata S, Usui E, Shiku H. Mutational analysis of the KIT gene in myelodysplastic syndrome (MDS) and MDS-derived leukemia. *Leuk Res* 2006; **30**: 1235–1239.
10 Padua RA, Guinn BA, Al-Sabah AI, Smith M, Taylor C, Pettersson T *et al.* RAS, FMS and p53 mutations and poor clinical outcome in myelodysplasias: a 10-year follow-up. *Leukemia* 1998; **12**: 887–892.
11 Reiter A, Sohal J, Kulkarni S, Chase A, Macdonald DH, Aguiar RC *et al.* Consistent fusion of ZNF198 to the fibroblast growth factor receptor-1 in the t(8;13)(p11;q12) myeloproliferative syndrome. *Blood* 1998; **92**: 1735–1742.
12 Deguchi K, Gilliland DG. Cooperativity between mutations in tyrosine kinases and in hematopoietic transcription factors in AML. *Leukemia* 2002; **16**: 740–744.
13 Loriaux MM, Levine RL, Tyner JW, Frohling S, Scholl C, Stoffregen EP *et al.* High-throughput sequence analysis of the tyrosine kinome in acute myeloid leukemia. *Blood* 2008; **111**: 4788–4796.
14 Sjoblom T, Jones S, Wood LD, Parsons DW, Lin J, Barber TD *et al.* The consensus coding sequences of human breast and colorectal cancers. *Science* 2006; **314**: 268–274.
15 Tomasson MH, Xiang Z, Walgren R, Zhao Y, Kasai Y, Miner T *et al.* Somatic mutations and germline sequence variants in the expressed tyrosine kinase genes of patients with *de novo* acute myeloid leukemia. *Blood* 2008; **111**: 4797–4808.

Supplementary Information accompanies the paper on the Leukemia website (http://www.nature.com/leu)

Rapid diagnosis of ataxia-telangiectasia by flow cytometric monitoring of DNA damage-dependent ATM phosphorylation

Leukemia (2009) **23**, 409–414; doi:10.1038/leu.2008.195;
published online 17 July 2008

Ataxia-telangiectasia (A-T) is an autosomal recessive disorder characterized by cerebellar ataxia, telangiectasias, immune defects and a predisposition to malignancy. The birth frequency of A-T is estimated to be about 1 in 100 000–300 000. The A-T heterozygote frequency is estimated to be 0.5–1%. The patient shows progressive cerebellar ataxia since infancy. Telangiectasia typically develops after 3–5 years of age. Sixty to 80% of patients show immunodeficiency. Twenty to 30% of patients develop a malignancy, mainly leukemia or lymphoma. Laboratory finding shows decreased level of serum IgA, IgG2 and IgE. Increased level of serum α-fetoprotein is a specific feature. Peripheral circulating lymphocytes show characteristic intra-locus rearrangements involving T-cell receptor and/or immunoglobulin loci. Chromosomal breakage and hypersensitization to ionizing radiation (IR) are a hallmark cell biological feature of the A-T cell. A-T cells also show improper cell cycle regulation after IR, which has been known as radioresistant DNA synthesis.

The responsible gene, ataxia-telangiectasia mutated (*ATM*), contains 66 exons spanning approximately 150 kb of genomic DNA at 11q22.3. cDNA contains 10 140 bp. The ATM protein contains 3056 amino acids coded by a 9168-bp open reading frame.[1,2] The ATM gene is also known to be mutated secondarily in various hematological malignancies, and is speculated to work as a tumor suppressor gene.[3] ATM protein is one of the members of phosphoinositide 3-kinase-related kinases. Exposure of cells to genotoxic stresses such as anticancer drugs or irradiation induces DNA double-strand breaks. The central player in such DNA damage response is ATM.[4] ATM is present as a dimer or higher-order multimer in unstressed cells with the kinase domain bound to the region surrounding serine (Ser) 1981. Cellular irradiation induces rapid intermolecular autophosphorylation of Ser 1981 and this phosphorylation event results in dimer dissociation and initiation of cellular ATM kinase activity.[5]

Diagnosis of A-T is based on clinical features combined with laboratory findings. Several cell biological and molecular approaches, such as protein truncation assay, yeast-based protein truncation assay, western blotting, RNA restriction finger printing assay, and others, have been used to reveal ATM mutation prior to straightforward genome sequencing.[2] However, there is no standard method that could be applied in clinical diagnosis, genetic counseling or carrier prediction. Here, we describe a novel method for A-T diagnosis using measurement of phosphorylation status of ATM by flow cytometry.

DNA damage response occurring in cells was monitored by measuring the phosphorylation level of ATM at Ser 1981 using the flow cytometry technique. Phosphorylation of ATM at Ser 1981 is the hallmark of ATM activation and can be detected by the anti-phospho-ATM-specific antibody 10H11.E12 (Cell Signaling, Danvers, MA, USA). Epstein–Barr virus (EBV)-transformed wild-type lymphoblastoid cell line (LCL-WT) was irradiated or treated with hydrogen peroxide (H_2O_2) to induce DNA damage. Dose-dependent phosphorylation of ATM was detected 1 h after irradiation or H_2O_2 treatment by flow cytometry. An irradiation dose of 0.5 Gy was sufficient to induce phosphorylation of ATM at Ser 1981 and the level of phosphorylation increased in a dose-dependent manner (Figure 1a). Phosphorylation of ATM was seen in cells treated with 0.1 mM H_2O_2, and the level of phosphorylation increased in a dose-dependent manner up to 0.5 mM.

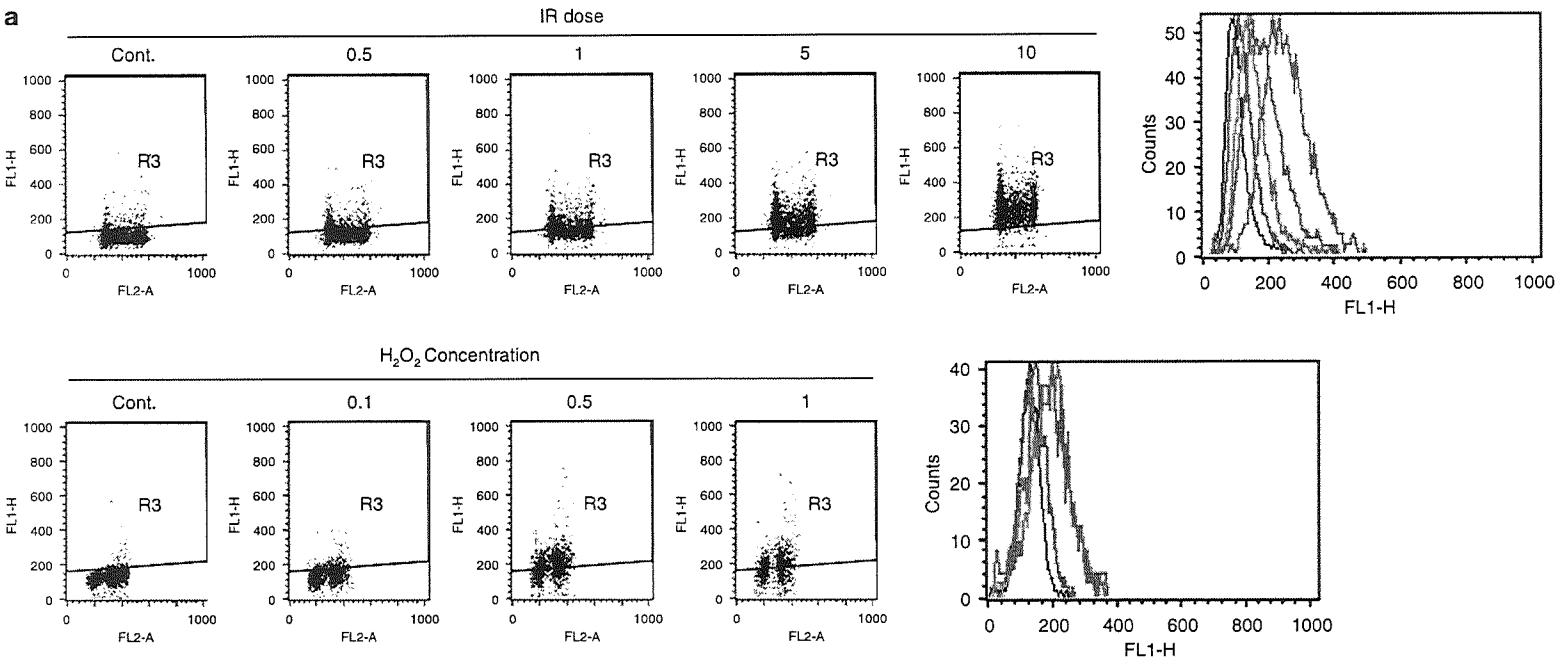

Figure 1 ATM phosphorylation status of LCL-WT detected by flow cytometry. (**a**) Upper panel: Irradiation induces ATM phosphorylation in a dose-dependent manner in LCL-WT. ATM phosphorylation was measured 1 h after irradiation. Radiation dosage is described above the dot blot gram. Right histogram panel corresponds to the results from dot blot gram. Black line: control, non-irradiated; red line: 0.5 Gy; green line: 1 Gy; pink line: 5 Gy; blue line: 10 Gy. Lower panel: H_2O_2-dependent ATM phosphorylation in LCL-WT. ATM phosphorylation was measured 1 h after H_2O_2 treatment. H_2O_2 concentration is described above the dot blot gram. Right histogram panels correspond to the results from dot blot gram. Black line: control, non-treatment; red line: 0.1 mM; green line: 0.5 mM; blue line: 1 mM. (**b**) Upper panel: Time kinetics of ATM phosphorylation after irradiation in LCL-WT. ATM phosphorylation was measured 10–60 min after 10 Gy irradiation. Time point when ATM phosphorylation was measured is described above the dot blot gram. Cont.: control non-treatment. Right histogram panels correspond to the results from dot blot gram. Black line: control, non-treatment; green line: 10 min; pink line: 30 min; blue line: 60 min. Lower panel: Time kinetics of ATM phosphorylation after H_2O_2 treatment in LCL-WT. ATM phosphorylation was measured at the indicated time points after H_2O_2 treatment. Right histogram panels correspond to the results from dot blot gram. Black line: control, non-treatment; blue line: 15 min; pink line: 30 min; green line: 60 min. (**c**) ATM phosphorylation status in ataxia-telangiectasia (A-T) LCL in comparison with LCL-WT. ATM phosphorylation was measured 1 h after 10 Gy irradiation, or 1 h after 1 mM H_2O_2 treatment in LCL-WT (upper panel) and AT52RM with ATM deficiency (lower panel). Right histogram panels correspond to the results from dot blot gram. Black line: control, non-treatment; red line: irradiated cell; green line: H_2O_2 treated cells.

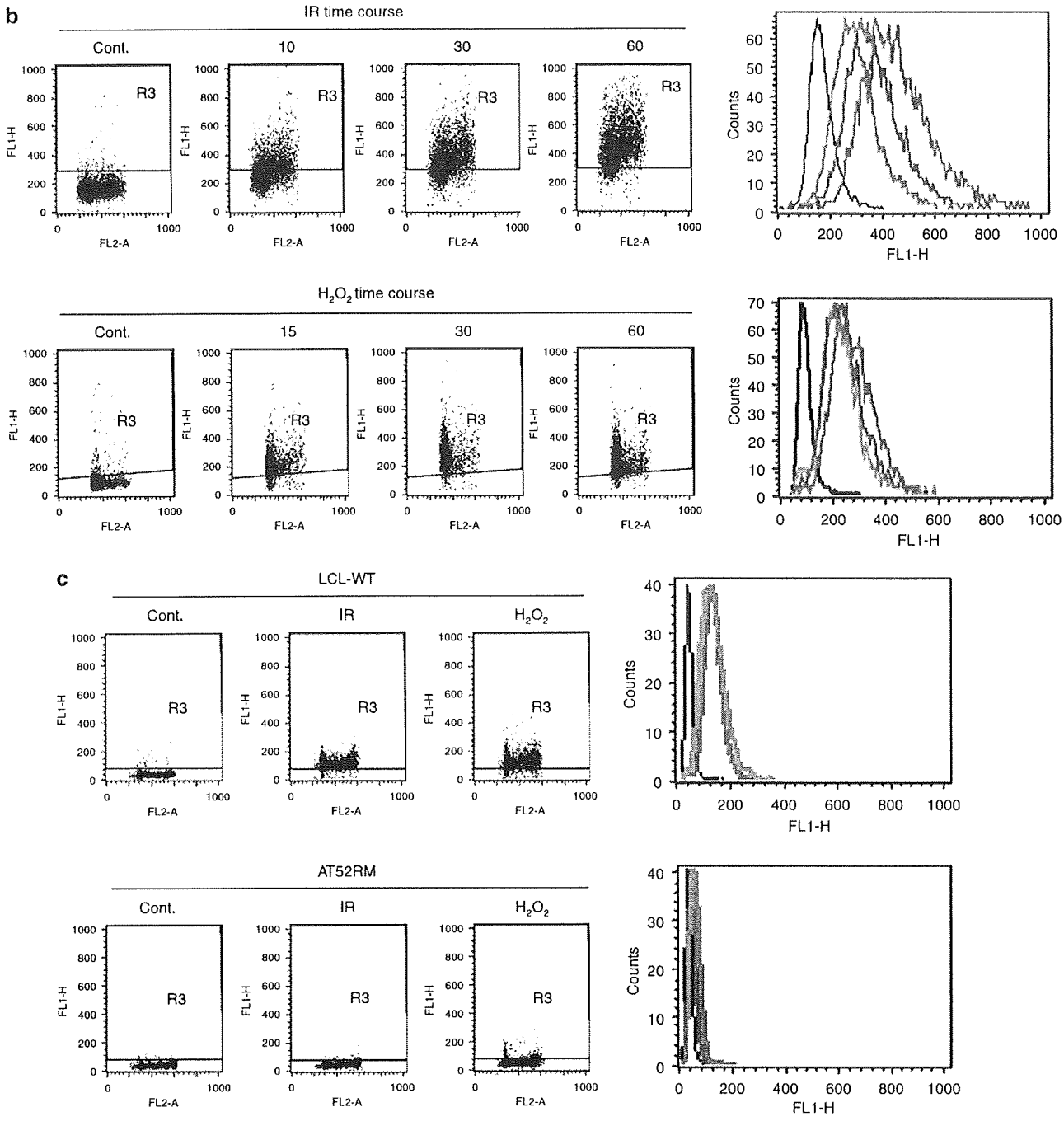

Figure 1 Continued.

Treatment with H_2O_2 appeared to reach plateau at the doses of 0.5 and 1 mM H_2O_2 based on the equivalent level of phosphorylation seen by flow cytometry (Figure 1a). Next, the time kinetics of ATM phosphorylation status was investigated in 10 Gy IR- or 0.5 mM H_2O_2-treated cells. ATM phosphorylation was detected 10 min after IR and 15 min after H_2O_2 treatment, and reached its near-maximum level at 60 min after IR and 30 min after H_2O_2 treatment (Figure 1b).

To validate the phosphorylation status demonstrated by flow cytometry in LCL-WT, the same assay was applied to AT52RM, an A-T LCL with null ATM expression by compound heterozygous truncation mutations 7626 C>T/8365 del A, and was compared with that in LCL-WT. Phosphorylation after 10 Gy IR and 0.5 mM H_2O_2 treatment was detected in LCL-WT but not in AT52RM (Figure 1c). These results are compatible with the interpretation that the phosphorylation detected by flow cytometry corresponds to ATM phosphorylation. This observation prompted us to investigate whether the flow cytometric monitoring of DNA damage response is applicable for A-T diagnosis in the clinical setting.

Peripheral blood mononuclear cells (PBMNCs) were cultured using media with 700 U/ml interleukin-2 (IL-2) and co-cultured with anti-CD3 antibody, which activates peripheral blood T cells (activated T cell)[6] and provides enough numbers of